Ecological Engineering 212 (2025) 107487

Contents lists available at ScienceDirect

Ecological Engineering

journal homepage: www.elsevier.com/locate/ecoleng

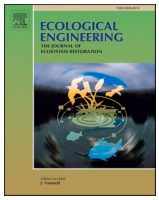

Comparative geotechnical analysis of slope stabilization through conventional, soil and water bioengineering, and combined solutions

Marco Uzielli [a,b,*], Andrea Geppetti [a], Lorenzo Borselli [c,d,e], Stefano Renzi [b], Federico Preti [f,g]

[a] Department of Civil and Environmental Engineering, University of Florence, Italy
[b] Georisk Engineering S.r.l., Florence, Italy
[c] Institute of Geology, Universidad Autónoma de San Luis Potosí, Mexico
[d] Consiglio Nazionale delle Ricerche, Istituto di ricerca per la protezione Idrogeologica (CNR-IRPI), Perugia, Italy
[e] Istituto Nazionale di Geofisica e Vulcanologia, Osservatorio Vesuviano, Napoli, Italy
[f] Dept. of Agricultural, Food, Environmental and Forest Sciences and Technologies, University of Florence, Italy
[g] AIPIN-EFIB (Italian Association and European Federation for Soil and Water Bioengineering), Italy

ARTICLE INFO

Keywords:
Geotechnical engineering
Bio-geotechnics
Slope stability
Soil and water bioengineering
Nature-based solutions
Statistics

ABSTRACT

The sustainable mitigation of hydrogeological hazard through the geotechnical stabilization of natural and artificial slopes is an ethical and technical goal of increasing global relevance. In this context, "gray" geotechnical stabilization solutions involving the use of inert materials, injections of cement mixtures and steel elements, have been prevalently used in the past decades and have thus come to define the present "conventional" approach. These solutions may meet engineering performance criteria but are unable to attain desirable sustainability standards. The practice of Soil and Water BioEngineering (SWBE) draws from ancient empirical experience and is rapidly gaining new momentum due to the increased focus on environmental protection and requalification. SWBE and can be effectively conducted through the design and implementation of nature-based solutions (NBS) by using living plants, alone or in combination with locally available materials, to improve the engineering performance of ecosystems while fostering an increase in their biodiversity and environmental value. The domain of applicability of NBS is limited to quasi-surficial instability phenomena, since the root systems which provide resistance to destabilizing forces are found mainly at shallow depths from ground surface. Moreover, biological and physical processes intervening in NBS result in the temporal variation of their mechanical resistance and engineering performance. "Combined" solutions involving the presence of – and synergy between - gray and green solutions may ensure the simultaneous attainment of safety and sustainability. This paper describes the conceptual standpoints and operational framework used for the comparative assessment of the engineering design performance of conventional, NBS, and combined solutions for a slope stabilization intervention on a site located near Florence, Italy. Stability is assessed quantitatively through limit equilibrium methods for multiple scenarios defined in terms of technological solutions, temporal stage, and level of engineering conservatism in design parameters. Temporal trends of the factors of safety against sliding are defined statistically and assessed qualitatively and quantitatively. The comparative analysis suggests that the combined solution provides the best option at the Montisoni site as it ensures sufficient short-terms, post-stabilization stability as well as increased stability overtime due to the improvement in the mechanical contribution of NBS components. The paper brings innovative contributions with respect to the equivalent geomechanical modeling of NBS and combined solutions in limit-equilibrium analyses and to the discussion of criteria to be considered in the assignment of design values in stability analyses.

* Corresponding author at: Department of Civil and Environmental Engineering, University of Florence, Italy.
E-mail addresses: marco.uzielli@unifi.it (M. Uzielli), andrea.geppetti@unifi.it (A. Geppetti), lorenzo.borselli@uaslp.mx (L. Borselli), sre@georisk.eu (S. Renzi), federico.preti@unifi.it (F. Preti).

https://doi.org/10.1016/j.ecoleng.2024.107487
Received 11 June 2024; Received in revised form 26 October 2024; Accepted 2 December 2024

1. Introduction

1.1. Ancient knowledge, new challenges

We live in times of rapidly evolving global awareness towards environmental and financial sustainability. Ethically oriented criteria are steering research and practice of technical and non-technical disciplines towards sustainable paradigms which strive to achieve sustainable development. In the domain of geotechnical engineering, efforts are increasingly focused on the development and implementation of innovative, nature-based, "green" solutions. This focus is well-motivated because high-risk scenarios are becoming more frequent and affect more human-valued assets. For instance, research increasingly indicates that climate change trends are expected to increase slope instability hazard in many parts of the world (e.g., Gariano and Guzzetti, 2016; Giachi et al., 2024; Uzielli et al., 2018). Geotechnical stabilization solutions conventionally involve the use of inert materials, injections of cement mixtures, and steel elements. These "gray" solutions, if appropriately designed, provide mechanical characteristics which are sufficient to ensure the desired engineering performance. However, they may not meet environmental sustainability criteria. Under certain physical and environmental conditions, it is possible to limit the use of such solutions and replace them with soil and water bioengineering (SWBE) interventions such as nature-based solutions (NBS). These use native living plants, alone or in combination with locally available materials (e.g., wood, soil, stones, geotextiles, galvanized steel mesh, etc.) to increase the hydro-mechanical performance of ecosystems while fostering their environmental sustainability. SWBE interventions are beneficial in terms of both mechanical and hydrological effects through a number of physical actions; more specifically: root reinforcement, plant-induced suction, canopy interception, runoff interception, and the self-weight of vegetation (e.g., Li et al., 2023). Root reinforcement is recognized as the main contributor of vegetation to slope stability. The complex multi-scale, and multi-directional structure of root systems brings an increase in the shear strength of soils by intercepting tension cracks and shear planes and resulting in increased aggregate cohesive and frictional properties.

The practice of SWBE through the design and implementation of NBS allows the simultaneous achievement of technical-functional, but also ecological, landscape and socio-economic goals to protect, sustainably manage, and restore natural and modified ecosystems, thereby benefiting people and nature. NBS are not a new product of human ingenuity. Plants and vegetation have been used to regulate hydraulic and erosional/instability phenomena on slopes over the centuries (e.g., Preti et al., 2022a, 2022b). Given the reawakening of awareness on sustainability, the use of NBS has experienced a momentous comeback in recent years and has begun permeating new domains, such as that of geotechnical engineering. Geotechnical research is focusing increasingly on NBS, and the recent coining of the term "biogeotechnics" attests to the surging interest towards environmentally sustainable solutions within the discipline. In a geotechnical perspective, NBS provide a promising means to achieve the dual objective of engineering performance and environmental sustainability. Research efforts and real-world applications are increasingly demonstrating that NBS can be cost-effective solutions for mitigating geotechnical risks associated with natural hazards (Capobianco et al., 2022). However, as with any other technological solution, NBS are not the solution to every problem. Their domain of applicability and their technical suitability with respect to specific problems should be well understood by designers prior to embarking on design efforts which may – or may not – reveal such limitations. In the context of slope stabilization, SWBE interventions are effective in the case of predominantly superficial or shallow instability phenomena, since the destabilizing forces must be balanced and absorbed by the resistance of the root systems of the plant species used, which exists prevalently in surficial soil layers (e.g., Preti and Giadrossich, 2009). Conventional measures are required for instabilities involving deep movements and high stress levels. Moreover, NBS are not applicable in slopes with predominant lithoid component and cannot thus be used in the mitigation of instability phenomena involving rocks and debris.

The domain of applicability of NBS can be extended through the use of combined solutions, which are physically composed of both conventional and nature-based elements. Combined solutions exploit the synergy of these solutions and their respective strengths to achieve an overall improved level of engineering performance and environmental sustainability. These solutions "combine the technical requirements of hydraulic safeguard or stabilization of a gravitational instability with the maximum possible conservation of the territory and its environmental value" (e.g., Sauli et al., 2005; Stokes et al., 2014; Rey et al., 2019). Numerous real-world applications have demonstrated the technical and financial advantages of resorting to combined solutions (e.g., NBRO, 2019; Fatahi et al., 2010).

The more immediate effectiveness of combined and gray measures is recognized and preferred, but generally combined measures with elements of gray and green are considered to be optimal for ensuring the temporal continuity of performance from the short- to the long-term. Another aspect that should not be overlooked concerns the subjective perception of combined solutions on the part of technical and non-technical stakeholders. Fig. 1 shows represents an overview of the main preference factors, obtained from a series of surveys, that influence the choice of the type of intervention to be carried out, in the common perception of engineering works: having assessed the technical requirements at first, these have to be complemented by many other aspects, such as construction time, cost, and the perception of risk (Anderson et al., 2022).

An additional factor which currently hinders the diffusion and use of NBS in geotechnical engineering practice is the difficulty in designing and analyzing the performance of soil-structure systems involving NBS solutions in accordance with current prevalent design formats. Notwithstanding the growing focus and awareness, geotechnical analysis and design of NBS are currently at a rather primal state due to relative paucity of experimental and empirical data, quantitative analysis methods, and code-compliant design modes. NBS have typically been designed in the past using empirical approaches and only a limited number of engineering approaches to the assessment of geotechnical performance are available (e.g., Acharya, 2018). Geotechnical analyses not strictly related to design, such as slope stability analyses, are also hindered by the lack of well-established approaches to the modeling of materials not amenable to natural geomaterials (soil, debris, rock). To further complicate matters, the strict application of current prevalent design formats would require the quantitative modeling of uncertainties to assign characteristic values. Geotechnical engineering deals with geomaterials and artificial materials (e.g., concrete, geosynthetics, etc.). Soil-structure systems are inherently complex due to aleatory uncertainty (spatial and temporal variability) and epistemic uncertainty (high statistical uncertainty due to limited quantity of data, high measurement uncertainty, high transformation uncertainty, high model uncertainty due to the many factors which intervene in achieving – or not achieving - design performance. As discussed in Section 4, geotechnical design codes are seldom applied consistently with their statistical character. The inclusion of NBS in geotechnical models introduces significant additional uncertainty, at least for two main reasons. First, the presence of materials with heterogeneous mechanical properties, typical failure behavior, and abrupt geometric discontinuities with respect to the natural soil stratigraphy can be expected to significantly increase modeling uncertainty. Second, NBS are affected by biological, chemical, and other physical processes which occur in their natural components. From a geotechnical perspective, these processes result in the temporal variability of their mechanical performance and of their interaction with geomaterials, thereby contributing to increasing aleatory and epistemic uncertainties.

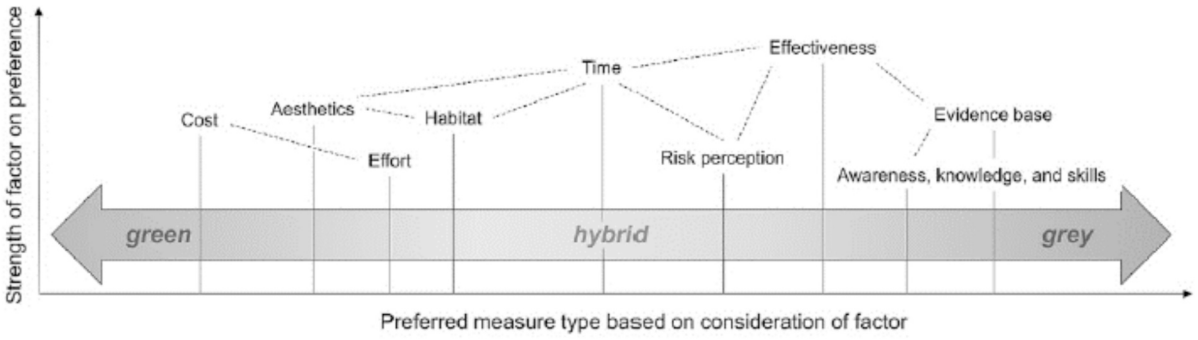

Fig. 1. Preferred types of interventions based on consideration of various preference factors (after Anderson et al., 2022).

1.2. Aim of study

This paper joins a currently limited corpus of technical literature (e.g., Bischetti et al., 2021) in advocating that the wider adoption of NBS and combined solutions by geotechnical practitioners can be facilitated and fostered through the development of guidelines, methods, and case-histories. To this purpose, the paper develops and describes the conceptual standpoints and operational framework used for the comparative assessment of the engineering design performance of conventional, NBS, and combined solutions for a slope stabilization intervention in Tuscany, Italy. The framework focuses on a set of fundamental specificities of the geotechnical approach to the analysis and design of NBS;

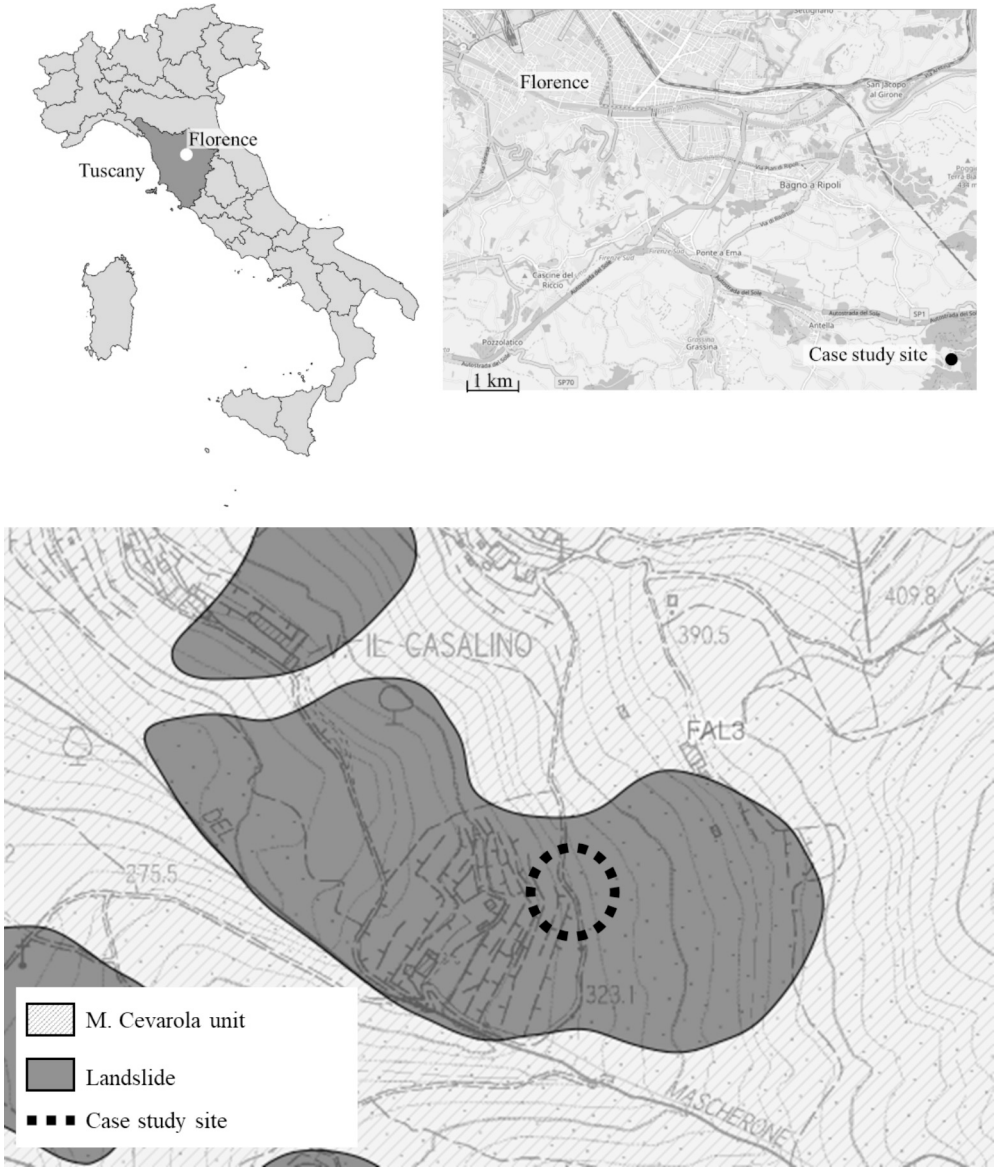

Fig. 2. Geographical and geological identification of the case-study site (re-elaborated from OpenStreetMap, 2024 and Regione Toscana - DB Geologico).

namely: (1) the technical suitability of different categories of technological solutions (i.e., conventional, NBS, combined); (2) the temporal variability of the performance of geotechnical systems involving the use of NBS and combined solutions; and (3) the criteria used to define representative values of geomechanical parameters. With respect to the last point, it is of interest to discuss the engineering assignment of modeling inputs in the light of currently prevalent design formats such as load-resistance factor design (LRFD) adopted, for instance, in the structural Eurocodes.

The paper brings innovative contributions with respect to the equivalent geomechanical modeling of slope stabilization solutions in limit-equilibrium analyses considering the specificities in conventional and NBS components. Moreover, the paper provides links between modeling choices and the conceptual foundations of LRFD approaches, which require the definition of "representative" (e.g., "characteristic values" in Eurocode 7). Slope stability is investigated quantitatively through a well-established and routinely adopted geotechnical engineering approach involving the use of limit equilibrium methods. The analyses and the assessment of the results are conducted for multiple scenarios defined in terms of technological solutions, temporal stage, and level of engineering conservatism in design parameters. Outputs are presented in both qualitative and quantitative formats to allow an enhanced understanding of the correspondence between physical phenomena and engineering outputs. Though the analysis is framed within a geotechnical standpoint, this paper wishes to emphasize and promote an interdisciplinary approach to the technical design and implementation of NBS in physical systems.

2. Case study presentation

The uniqueness of physical systems and the site-specificity of their geometric and geotechnical attributes do not allow the conduct of analyses of general validity. This paper focuses on a case study located in Via di Montisoni, a historic rural road in a prized landscape value area surrounding the city of Florence (Fig. 2). The case study refers to a slope instability event classifiable as a compound phenomenon based on the Varnes (1978) system, which occurred in the month of November 2020 following heavy rainfall (Fig. 3).

Based on the climate classification of Köppen and Geiger (1954), the climate in the investigated area is Mediterranean, temperate, and moderately humid but with dry and relatively hot summers. Rainfall is typically Mediterranean and characterized by low rainfall summers. The maximum rainfall peak occurs in November with an average of 135 mm approximately, while the minimum rainfall is in July, with an average of 30 mm approximately. The total yearly rainfall is 800 mm, approximately. Morphologically, reliefs are hilly, with gentle and rounded shapes. The section of the road affected by instability lies at an elevation of about 325 m asl. Slope angle varies between 15° and 25°. The slope is locally terraced with alternating sub-horizontal shelves and sub-vertical dry-stone walls. The section of road investigated is located on a west-facing hillside with a high-value view on the city of Florence and runs through privately owned agricultural land punctuated by olive groves (West) and woodland (East). From the geo-lithological point of view, the area is located on the Mount Cervarola Tectonic Unit, Montalto Member, with overlying pedological, debris, and colluvial covers in the first 2-3 m below ground surface and with the presence of silicoclastic turbiditic sandstones, in predominantly arenaceous-pelitic facies (Cervarola Sandstone Formation). These covers are sandy-loamy, brown in color, with organic matter and stone fragments. Surficial covers are altered and moderately degraded, mainly due to their organic content. The underlying lithoid substrate displays limited alteration and a medium degree of fracturing. The arenaceous-silitic formations host aquifers of moderate importance in the fractures of lithoid horizons. Surface covers in the area are occasionally traversed by seepage water and underground circulation. Specifically, it has been assessed that in the presence of prolonged rainfall, a stable, albeit ephemeral, water circulation may be established that can influence slope stability conditions. This phenomenon is thought to have been the main triggering factor of the 2020 event. Wells in the area reveal the presence of aquifer bodies at depths 30-40 m below ground level within the Cervarola sandstone formation. The geotechnical characterization of the site relied on two dynamic penetrometer super-heavy tests (DPSH) with depth 3.4 and 4.6 m and located near the road and up-hill of the road, and two MASW geophysical refraction tests. Further details of the geotechnical characterization process are available in Boni (2022).

From a vegetational perspective, the area many of the typical species

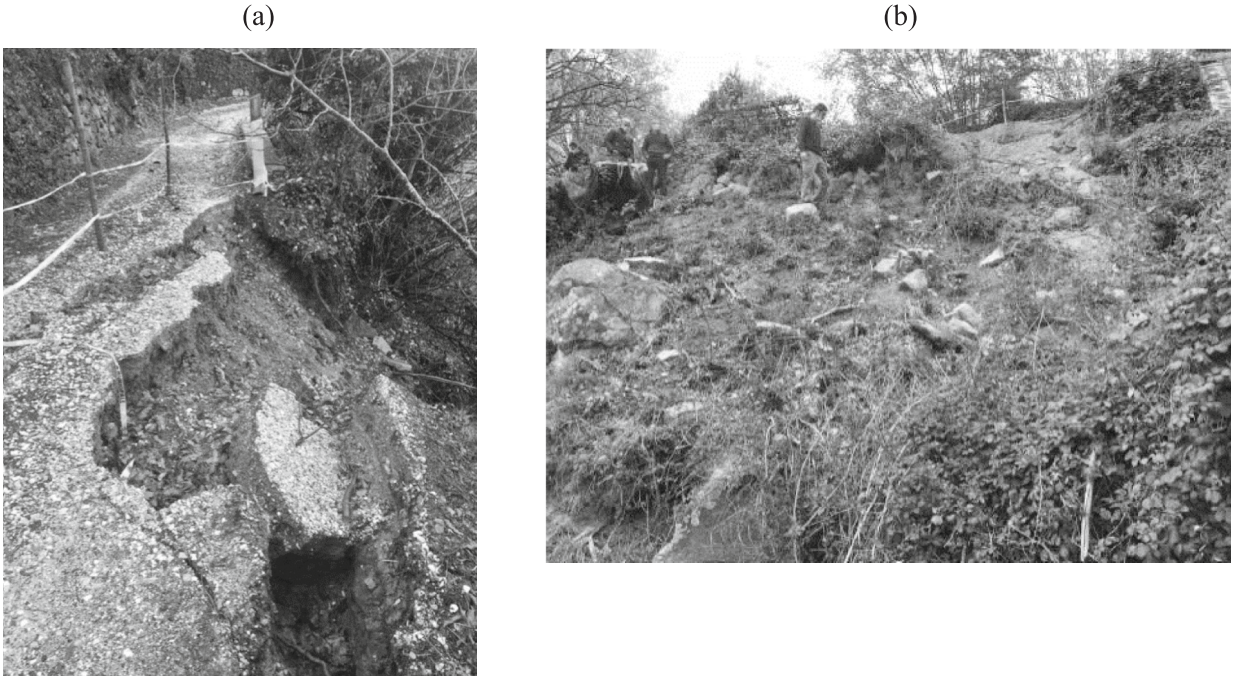

Fig. 3. The 2020 Montisoni landslide: (a) view from the road; (b) view from downslope.

of Mediterranean deciduous forest such as oaks (holm oak, downy oak, turkey oak, downy oak), other broadleaf types (ash, maple, chestnut, alder, poplar, black hornbeam, white hornbeam, linden, wild cherry, walnut, hazel, rowan), and conifers (red juniper, Phoenician juniper). An on-site survey revealed a modest component of tree vegetation, accompanied by dense undergrowth in which a wide variety of herbaceous and shrub species including *Castanea sativa*, *Juglans regia*, *Ostrya carpinifolia*, *Pinus Halepensis*, *Quercus ilex*, and *Quercus pubescens*.

The stabilization of the slope involved the design and the sequential implementation of the following technical interventions: (1) reinstatement of the road embankment in order to create a safe working surface for the laying of minipiles (Fig. 4a); (2) realization of a drainage trench and a microfissured pipe with water drainage function on the upslope side of the road (Fig. 4a); (3) realization of a row of 11 steel minipiles on the downslope side of the road (Fig. 4b),connected by a concrete cap and each having a length of 8.00 m, a drilling diameter of 200 mm, an external diameter of 114.3 mm, a thickness of 8 mm, a yield stress of 355 N/mm^2, and an inter-axial spacing between consecutive piles of 0.75 m.; (4) reprofiling of the slope by means of two orders of double piles and wooden crib walls, filled with excavated soil and draining material in order to lower groundwater level (Fig. 4c and Fig. 4d); (5) greening of the slope by planting a mixture of grasses and legumes including *Prunus*, *Digitaria sanguinalis*, *Spartium junceum*, *Laurus nobilis*, *Fraxinus ornus*, and *Carpinus betulus* (Fig. 4e); and (6) construction of retaining wall on the downslope edge of the road and construction of white road and transverse and longitudinal drainage channels (Fig. 4f).

In order to identify experimentally the most effective building technique for the live crib wall, two approaches were adopted, respectively, for the first and the second order. Transverse wooden piles were assembled *inline* (i.e., with piles in phase at all levels) in the first order and "*a quinconce*" (i.e., with piles alternating at each level) in the second one. Moreover, bark was maintained on the longitudinal and transverse wooden piles in the first order, while stripped piles were used in the second order. The drainage behind the live crib wall was realized using a prefabricated system (Gabbiodren ®) for the first and with natural stones second order.

3. Geotechnical slope stability analysis

3.1. Analysis approach

The geotechnical assessment of slope stability requires the definition of a suitable "geotechnical model" accounting for the geometric, geomechanical, and hydrogeological attributes of a system. The geotechnical modeling of physical systems involving NBS is challenging because geotechnical tools and software developed for slope stability analysis require the "equivalent" modeling of materials which cannot be physically amenable to geomaterials, and who behavior at ultimate limit states may be very different from that of soils and rocks. The set of parameters included in a geotechnical model depends on the analysis approach adopted on a case-specific basis. Geotechnical slope stability analyses can be conducted using limit equilibrium methods (LEM) or numerical methods (e.g., finite-element methods, finite-difference methods, material point methods, etc.). In extreme synthesis, LEM relies on simplified two-dimensional geometric assumptions and simplified hypotheses regarding stress-strain states.

This paper relies on the LEM approach to slope stability. The LEM method was chosen for several reasons. First, it is the most well-known and frequently used method by designers. Since one of the aims of this paper is the provision of practical guidelines for the geotechnical modeling of slopes including conventional, nature-based, and combined stabilization solutions, it is conceptually pertinent to refer to practice-oriented tools. Second many design codes (e.g., the Italian NTC2018) require the conduction of LEM analyses even if other approaches are adopted. LEM methods rely on the analysis of static limit equilibrium conditions of one or more infinitely rigid bodies into which the soil mass is decomposed. Analyses are conducted on two-dimensional cross-sections assuming plane strain and simultaneous rupture along a specific sliding surface. Numerical methods allow, in principle, a more realistic and detailed modeling of the stress-strain phenomena occurring within a slope through the use of more sophisticated constitutive models and can allow the real three-dimensionality of slopes to be considered. However, the full exploitation of the potential of numerical analyses is almost invariably hindered, in real applications, by limited and insufficient geotechnical site characterization which impedes the adequate modeling of the spatial variability and uncertainty in geomechanical properties and, consequently, the rational calibration of constitutive models.

LEM methods do not include the evaluation of stress and deformation states but provide quantitative outputs in terms of the factor of safety (*FS*) against slope instability, given by the ratio of the shear strength of a soil along a specific sliding surface, τ_f, to the shear stress mobilized along the same surface, τ_m:

$$FS = \frac{\tau_f}{\tau_m} \tag{1}$$

Despite their fundamental simplifying assumptions, LEM analyses have been shown to provide reliable outputs if they are used rationally. The analyses pertaining to this study were conducted using the SSAP software (Borselli, 2023), which can be freely downloaded from https://www.ssap.eu. One of the main strengths of SSAP is the possibility of discarding aprioristic assumptions about the shape of the sliding surfaces (e.g. limited to only circular shape) and of generating slip surfaces randomly through advanced algorithms. This feature is especially relevant for systems involving NBS, which are geometrically complex, present strong discontinuities in geomechanical properties, and for which the assumption of circular or logarithmic slip surfaces are unrealistic. Moreover, SSAP provides a wide range of modeling options specifically pertaining to: (1) the inclusion of artificial and natural materials representing well-established and innovative stabilization solutions; (2) the generation of spatialized values (and maps) of *FS* using non-LEM procedures which allow the calculation of distribution of stress states. The following sections illustrate salient aspects of the main steps involved in the construction of the geotechnical models used in the case study application.

3.2. Stratigraphic modeling

The geometric definition of the geotechnical model (in the 2D case, a reference cross-section) to be used in LEM stability using the SSAP software analysis relied on the outputs of the geological, geotechnical, and hydrogeological characterization of the site described in Section 2. In accordance with such process, the geotechnical model of the site included four geomaterials were identified; namely: (1) a surficial layer of soil and colluvium altered by shallow sliding phenomena; (2) non-altered soil and colluvium; (3) Cervarola sandstone; and (4) debris. Fig. 5 shows the post-event, pre-stabilization cross-section indicating the markedly two-dimensional stratigraphic profile of the site. As multiple technological solutions were analyzed comparatively, different geometries were defined as inputs to SSAP for the post-stabilization phase. These are addressed in greater detail in Section 4.

3.3. Hydrogeological modeling

No specific information regarding the fluctuation of groundwater level was available for the slope. Hence, the most conservative scenario, in which the groundwater level coincides with the post-event topographic surface, was used in stability analyses. This approach is consistent with the provisions typically given in geotechnical design codes. For instance, clause 6.3.4 of the Italian technical code (NTC2018) states that when site-specific conditions do not allow easy evaluation of pore pressures, safety checks must be performed by assuming the most

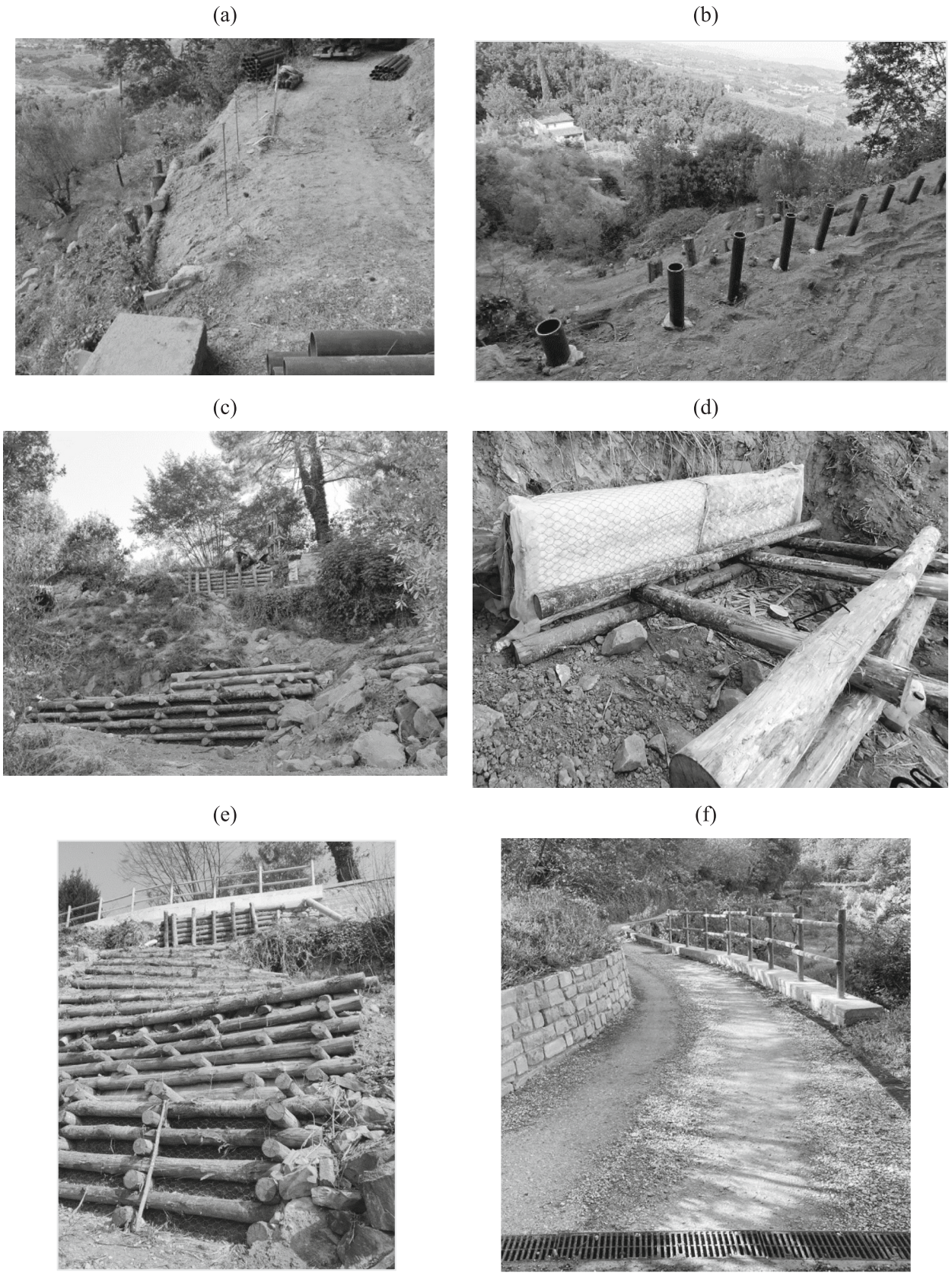

Fig. 4. Stabilization of the Montisoni landslide using a combined solution: (a) phases 1–2; (b) phase 3; (c) and (d) phase 4; (e) phases 5; (f) phase 6.

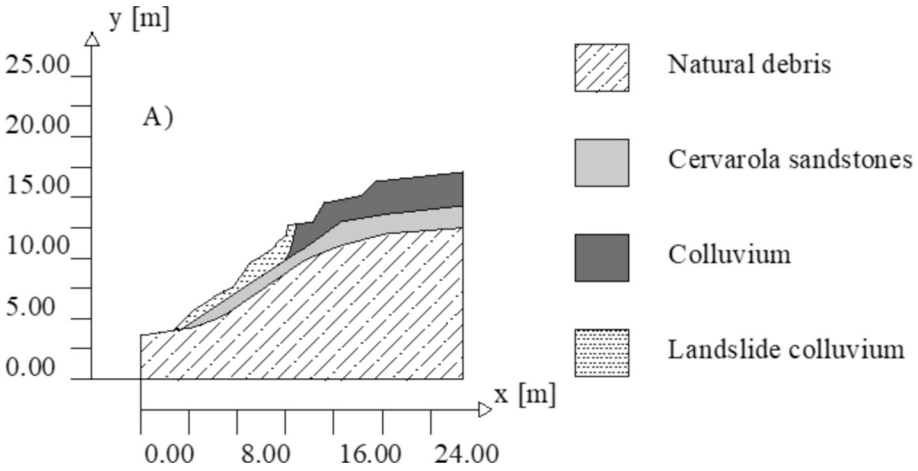

Fig. 5. Stratigraphic model of the Montisoni site after the landslide and before interventions.

unfavorable conditions that can be reasonably predicted. Clause 6.8.2 follows up by stating that, in the case of structures on slopes, the influence of the structure on the general safety conditions of the slope must be examined by taking into account the induced changes in pore pressures.

3.4. Geomechanical modeling

This section details the hypotheses and process underlying the assignment of geomechanical parameters to the geotechnical model of the Montisoni site to the purpose of LEM analyses. Such process relies partly on existing literature findings but provides an innovative articulate framework for addressing conventional, NBS, and combined stabilization solutions through the adoption of specific failure criteria and the definition of quantitative models for the assignment of parameters which are consistent with the physical attributes of each type of solution.

3.4.1. Equivalent geomechnical modeling of rooted soils

The ultimate limit-state behavior of rooted and non-rooted geomaterials in terms of shear stress was conducted by adopting the Mohr-Coulomb criterion by which mobilized shear stress τ_m (which, at failure, is equal to shear strength) can be expressed as the summation of a frictional and a cohesive component:

$$\tau_m = c' + (\sigma - u)tan\phi' \tag{2}$$

in which c' is the effective cohesion, σ is the total normal stress, u is the pore pressure, and ϕ' is the effective friction angle. The effect of the presence of vegetation on slope stability can be investigated in a geotechnical perspective through the adoption of appropriate constitutive models. Models for estimating root reinforcement of soils have been developed at an increasing pace since the 2000s, starting with the pioneering works of Waldron (1977) and Wu et al. (1979) and achieving milestones such as the Fiber (root) Bundle Model type (Preti, 2006; Schwarz et al., 2013; Murgia et al., 2022; Lann et al., 2024), eco-hydrological models (Preti et al., 2010; Gonzalez-Ollauri et al., 2021) and indirect models relying on the outputs of non-invasive methods (Giambastiani et al., 2021; Giachi et al., 2024). A systematic overview is provided in Mao (2022). Following a critical assessment of the methods, the SWWM-Wu-Preti approach was adopted. This approach has been extensively tested and validated (e.g., Preti, 2006; Schwarz et al., 2010; Ji et al., 2020), is more usable in practice than RBM (Root Bundel Model) or FBM (Fiber Bundle Model) methods which require the knowledge of a higher number of parameters (Schwarz et al., 2010; Gonzalez-Ollauri et al., 2021), and is compatible with the Mohr-Coulomb failure criterion given in Eq. (1) and opportunely modified by breaking down the effective cohesion term c' as:

$$c' = \varepsilon_{wsv} c_w(t) + [1 - \varepsilon_{wsv}][c_s + c_v(t,z)] \tag{3}$$

in which ε_{wsv} is the fraction of unit volume of lens pertaining to the wood-soil-root system, $c_w(t)$ is the time-dependent wood cohesion c_s is the depth- and time-invariant soil cohesion; and $c_v(t,z)$ is an additional, depth-time dependent cohesion brought by roots. The root-induced cohesion can be expressed as

$$c_v(t,z) = k_1 \bullet k_2 \bullet t_R(t,z) \tag{4}$$

where $t_R(t,z)$ is the depth- and time-dependent root tensile strength mobilized per unit area of soil and k_1 and k_2 are auxiliary coefficients (Mao, 2022). The mobilized tensile strength $t_R(t,z)$ can be calculated as the product of the average root tensile strength T_R and the root area ratio RAR:

$$t_R(t,z) = T_R \bullet RAR(t,z) \tag{5}$$

The root area ratio is defined as

$$RAR(t,z) = \frac{A_r(t,z)}{A_{soil}} \tag{6}$$

in which $A_r(t,z)$ is the aggregate cross-sectional area of the roots at a given temporal instant and depth z; and A_{soil} is the total time- and depth-invariant cross-sectional area of the rooted soil. Empirical observations indicate that root area increases over time and decreases with depth from ground level z according to the negative exponential relationship (Preti et al., 2010; Tron et al., 2014; Arnone et al., 2016; Preti et al., 2022b):

$$A_r(t,z) = A_{r0}(t) \bullet exp\left(-\frac{z}{b}\right) \tag{7}$$

where $A_{r0}(t)$ is the root area (increasing over time) at the surface and b is the average root depth, estimated as

$$b = \frac{\alpha}{AWC\left(1 - \frac{1}{DI}\right)} \tag{8}$$

in which α is the average intensity of rainfall events (in mm/event), AWC is the available water (in mm), and $DI = \frac{T_p}{(\lambda_0 \bullet \alpha)}$ is the Budyko Dryness index in the vegetative growth, where T_p is the fraction of potential evapotranspiration (in mm/day) and λ_0 is the average frequency of rainfall events (in events/day).

The Mohr-Coulomb failure criterion given in Eq. (3) can thus be reformulated as

$$\tau_{sr}(t,z) = \varepsilon_{wsv} c_w(t) + [1 - \varepsilon_{wsv}][c_s + c_v(t,z)] + (\sigma - u)\tan\phi' \quad (9)$$

in which shear strength is thus time- and depth-dependent due to the reasons discussed above.

The temporal increase and depth-wise decrease in $c_v(t,z)$ was modeled quantitatively by applying least-squares regression on an extensive database of measurements of root systems of 19 trees taken after the occurrence of approximately 800 landslides in mountainous and hilly areas of northern Tuscany. Details of the database can be found in Preti et al. (2022b), Preti et al. (2010), and Tron et al. (2014). In the Montisoni case-study, a "sandy loam" soil type was assumed. The auxiliary coefficient k_1 was introduced by Waldron (1977) and Wu et al. (1979) and quantifies root orientation, taking values between 1.0 and 1.3 with increasing deviation from perpendicularity to the sliding surface. The coefficient k_2 is an empirical correction factor, conventionally taken as 0.4 (Preti, 2006; Schwarz et al., 2010; Mao, 2022), which accounts for the overestimation in cohesion values obtained by the method proposed by Wu et al. (1979).

The spatial variability of equivalent cohesion was accounted for in LEM analyses by defining layers which are geometrically parallel to the topographic surface from ground level. More specifically, three layers of thickness 0.50 m, 0.50 m, and 0.20 m starting from ground level were defined for the live crib walls, and two layers of equal thickness 0.50 m were defined for the live grids. Following this approach, values of equivalent cohesion were obtained for the end-of-construction temporal stage.

For the simulation of the wood-soil-root system, a value of ε_{wsv}=0.2 was assumed based on expert judgement. As is typically the case for NBS implementations, the temporal evolution of the mechanical characteristics of the geotechnical system is expected to be of paramount importance in the Montisoni case study due to: (a) the progressive degradation of the wooden parts of the live crib walls and the wooden poles; (b) the progressive growth of root systems. These phenomena cause contrasting variations in terms of the mechanical behaviors and of the overall stability of the geotechnical system: the degradation of wooden elements reduces mechanical resistance while the growth of roots brings additional strength to soils (e.g., Sauli et al., 2005; Preti et al., 2011; Romano et al., 2016). It is not possible to assess a priori the aggregate effect of these variations and to identify the most severe temporal stage for the system. Good practice thus warrants the conduction of stability analyses at multiple temporal stages (Bischetti et al., 2021). To this purpose, ten stages were identified for the case study; namely: end of construction; and 1, 2, 3, 4, 5, 10, 15, 20, and 25 years following construction. A greater temporal resolution was adopted for the 5 years following construction to assess in greater detail the post-stabilization short-term effects of soil rooting.

Representative values of c_v were assigned to each layer by calculating through the evaluation of the integral (of the cohesion function with depth) weighted over the thickness of the layer by applying the analytical model in Eq. (5) to the depth intervals corresponding to each layer. Fig. 6 shows the depth-wise and temporal variation of c_v for five (i.e., 5, 10, 15, 20, and 25 years) of the ten temporal stages considered in the analysis along with the representative values calculated at mid-depths below ground level (bgl) of the three live crib wall layers. A similar procedure was adopted to the layers used to model live grids.

3.4.2. Equivalent modeling of lens layers

Both conventional (minipiles) and nature-based (live crib walls, live grids) structural elements considered in the analysis interact with soils and their geotechnical design must account for such interactions. For instance, the behavior of the "minipile-soil" interaction is to be considered and investigated as to identify a spacing between minipiles which may allow the occurrence of the "arch effect" and avoid soil flow. The synergy between (conventional and nature-based) structural elements and soils can be conveniently modeled in SSAP as "lens layers". These are polygons that define the limits of specific geotechnical units

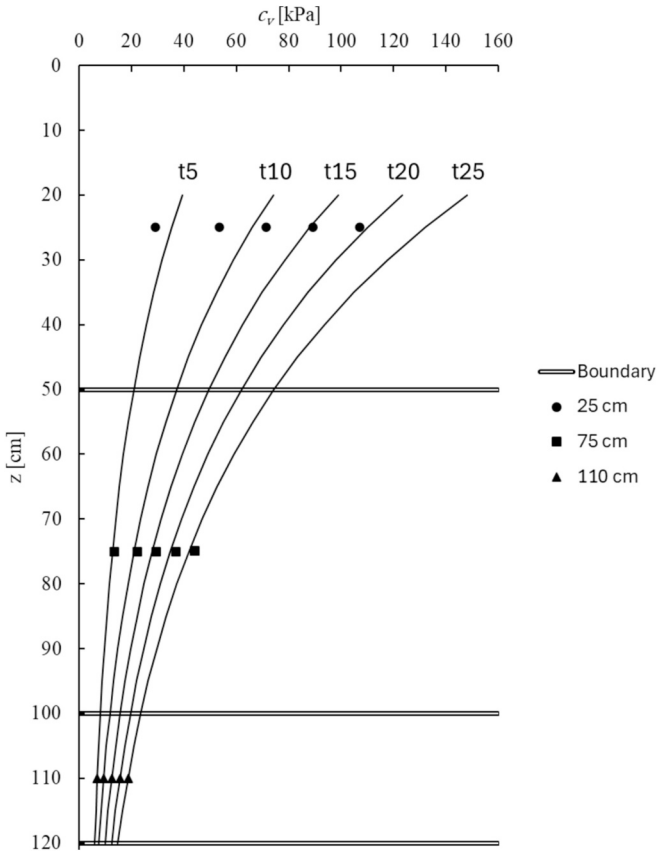

Fig. 6. Vertical spatial variation of root cohesion c_v for the t05, t10, t15, t20, and t25 temporal stages for live crib walls and live grid lenses.

which can be completely enclosed inside other layers.

The equivalent geomechanical modeling of the lens layers was conducted following a critical assessment of their expected mechanical behavior and temporal variability. The three main statements which can be made are: (1): the aggregate mechanical behavior can be assigned quantitatively as a function of the individual mechanical behaviors of the materials constituting the composite lens materials; (2) the physical attributes of the lens layers considered in the study do not involve any frictional component of strength; and (3) the degradation of conventional materials (steel, concrete) occurs over a temporal period which is much longer than the maximum temporal stage considered in this study (25 years), while the degradation of wooden structural elements is significant over this temporal span. Point (1) suggests the use of a general model for estimating equivalent geomechanical parameters of lens layers as

$$\Omega_{eq.lens} = \varepsilon\Omega_{mat} + (1 - \varepsilon)\Omega_{soil} \quad (10)$$

in which $\Omega_{eq.lens}$ is the equivalent value of a generic geotechnical parameter; Ω_{mat} and Ω_{soil} are the values of the same property pertaining to the structural elements and the soil, respectively; and ε is the fraction of unit volume of lens pertaining to the structural element. Point (2) suggests that the ultimate limit-state behavior of lens layers was modeled by adopting the Tresca failure criterion. In its original formulation, the Tresca criterion defines the shear strength of a material as being equal to its cohesion s_u:

$$\tau_m = s_u \quad (11)$$

Point (3) suggests that the equivalent modeling of the minipile and wooden pile lenses should account for the specific attributes of the cohesive mechanical behavior of the individual components of the composite lenses. Using the weighted model given in Eq. (10), the Tresca

criterion can be rewritten for minipile-soil lenses as

$$\tau_{m,mp} = s_{u,mp} = \varepsilon_{mp} s_{u,mp} + (1 - \varepsilon_{mp}) s_{u,s} \quad (12)$$

in which $s_{u,mp}$ is the equivalent shear strength of the minipile lens, ε_{mp}=0.31 is the minipile-soil volumetric ratio, $s_{u,mp}$ is the shear strength of the minipile, and $s_{u,s}$ is the undrained strength of the soil. All parameters appearing in Eq. (12) are time-invariant because no NBS are included in the lens. For the wooden pile-soil lenses, the Tresca criterion becomes

$$\tau_{m,wp}(t) = s_{u,wp}(t) = \varepsilon_{wp} s_{u,wp}(t) + (1 - \varepsilon_{wp}) s_{u,s} \quad (13)$$

in which $s_{u,wp}(t)$ is the equivalent shear strength of the minipile lens, ε_{wp}=0.196 is the wooden pile-soil volumetric ratio, $s_{u,wp}$ (t) is the time-variant (due to degradation) shear strength of the wooden pile, and $s_{u,s}$ is the undrained strength of the soil. Volumetric ratios ε_{mp} and ε_{wp} were assigned on the basis of the geometric and dimensional features of the respective models (i.e., diameters of design minipiles and wooden piles, design spacing between consecutive minipiles). The selection of an initial value of shear strength of chestnut wood used at the Montisoni site was conducted by referring to Eurocode 3 EN 1993-1-1:2005 (CEN, 2005). The temporal variation of equivalent parameters for NBS lenses was modeled by referring to the cohesion of rooted soils and the cohesion of the wooden elements of the live crib walls and of the live grids. The latter was assigned on the basis of an expert-based procedure involving the assignment of an initial value and a rule for temporal decrease which parameterized the progressive degradation of the wood. The definition of the trend of temporal degradation of wooden pile strength relied on the hypothesis by which the cohesion of wooden materials decreases linearly to halve its initial value over a period of 25

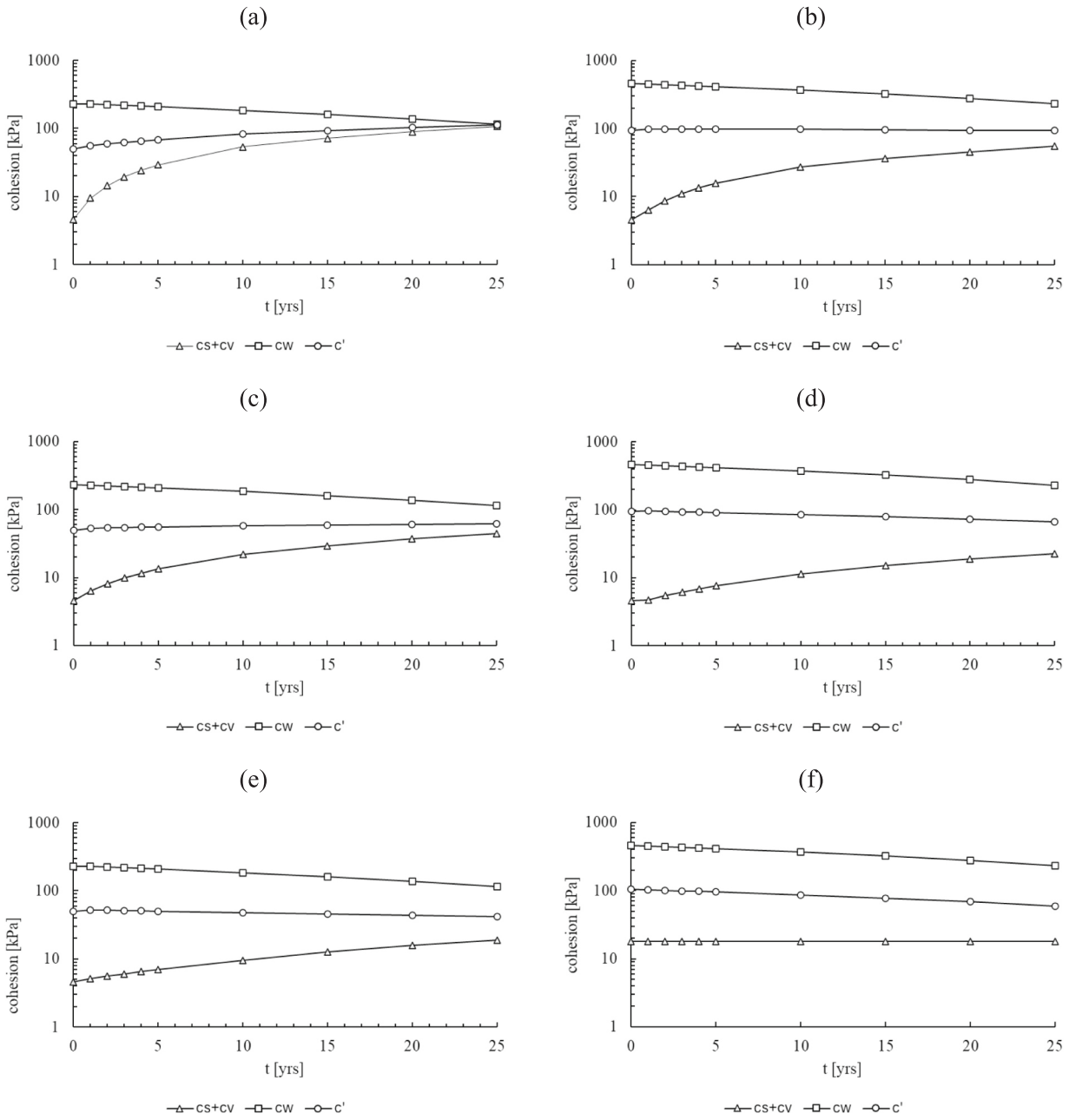

Fig. 7. Temporal evolution of wood cohesion and equivalent cohesion of NBS lenses at depths of: (a) 25 cm bgl for live crib walls and live grid lenses; (b) 25 cm bgl for the wooden pile lenses; (c) 75 cm bgl for live crib walls and grids lenses; (d) 75 cm bgl for the wooden pile lenses; (e) 110 cm bgl for live crib walls and grids lenses; (f) 270 cm bgl for the wooden pile lenses.

years. Such hypothesis is supported by past evidence (e.g., Mugnai, 2019; Perugini, 2010; Selli and Guastini, 2014) and is purposely conservative since it entails the inevitable simplification of complex three-dimensional patterns of spatial and temporal variability of mechanical properties of wooden structural elements of NBS. The resulting temporal variation of the effective cohesion of wood $c_w(t)$, of the rooted soil $c_v(t,z)$, and of the equivalent effective cohesion of NBS materials $c_{eq,NBS}$ are shown in Fig. 7 at significant spatial locations. More specifically, Fig. 7a refers to values calculated at 25 cm bgl (midpoint of the top layer of live crib walls and grid lenses); Fig. 7b refers to values calculated at 25 cm bgl (midpoint of the top layer of the wooden pile lens); Fig. 7c refers to values calculated at 75 cm bgl (midpoint of the intermediate layer of live crib walls and grid lenses); Fig. 7d refers to values calculated at 75 cm bgl (midpoint of the intermediate layer of the wooden pile lens); Fig. 7e refers to values calculated at 110 cm bgl (the midpoint of the bottom layer of live crib walls and grid lenses); and Fig. 7f refers to values calculated at 270 cm bgl (the midpoint of the bottom layer of the wooden pile lenses). It is interesting to note that the equivalent cohesion of the NBS lens increases over time for the live crib walls and live grids while it decreases for the wooden pile. The different behavior is due to the varying aggregate effect of the two factors appearing in the equivalent cohesive strength model; namely, the depth- and time-dependent variation in the cohesion of rooted soils $c_v(t,z)$, and the volumetric ratio ε which appears in such model. The temporal decrease in the equivalent cohesion of the wooden pile $s_{u,wp}(t)$ suggests the opportunity of periodically replacing wooden piles. The equivalent, time-invariant unit weights of lens layers was also calculated using Eq. (10). Further details of the geomechanical modeling process and are available in Boni (2022).

4. Definiation of modeling scenarios

Following the definition of the geotechnical models, the comparative analysis of slope performance was set up for LEM modeling scenarios defined by the physically plausible combination of: (1) stabilization technology solutions; (2) temporal stage of analysis; and (3) design mode.

4.1. Technological solutions

Solution A corresponds to the post-event, pre-construction state, with the post-event slope profile. Solution B corresponds to stabilization with only the conventional solution. In this case, the stabilizing effects of the row of minipiles are modeled following the Ito et al. (1981) methodology as implemented in SSAP (Borselli, 2023). The row of passive minipiles generates an arc-effect which induces a stabilizing reaction directed upslope, enhancing stability. The passive reaction force upslope is considered in the LEM procedure for the numerical computation of the factor of safety calculated using the Morgenstern and Price (1965) method. This method was chosen among other rigorous LEM methods available in the SSAP software because it is considered as one of the most numerically stable and of general applicability (Duncan, 1996; Chowdhury et al., 2009). The local shear strength effect of the minipile lens modeled using Eq. (10) should also be added to the passive pile effect when the minipiles are intersected by a potential sliding surface. Solution C1 involves stabilization exclusively with NBS solutions, consisting of: (a) 2 rows of 3 live crib walls, placed at the foot of the slope, and live grids, placed in the upper part of the slope. Solution C2 corresponds to the as-built state, i.e., with the combined solution including minipiles, live crib walls, and live grid. Solution D1 constitutes the evolution of solution C1, with the addition of a berm of wooden (chestnut) wooden poles, placed in the center of the live grid and reaching a depth of 4 m below ground level. Analogously, with respect to solution C2, solution D2 involves the addition of wooden poles. Technological solutions are shown schematically in Fig. 8.

4.2. Temporal stages

Current design codes largely neglect the importance of the temporal evolution of soil-structure system. In the modeling of retaining works, the Italian design code NTC18 “Update of the Technical Standards for Construction” (MIT, 2018), for instance, requires geotechnical verification of stability under static conditions solely at the end of construction. As mentioned previously, temporal variability plays a central role in the planning, design, and monitoring of NBS and combined solutions. The multiple temporal stages considered in the study are expected to cover the initiation, evolution, and completion of new root propagation.

4.3. Design modes

Geotechnical design codes are experiencing a shift in paradigm from the traditional deterministic approach to non-deterministic approaches in which uncertainties are accounted for explicitly in the design process. Currently, prevalent design codes such as the European Eurocodes adopt

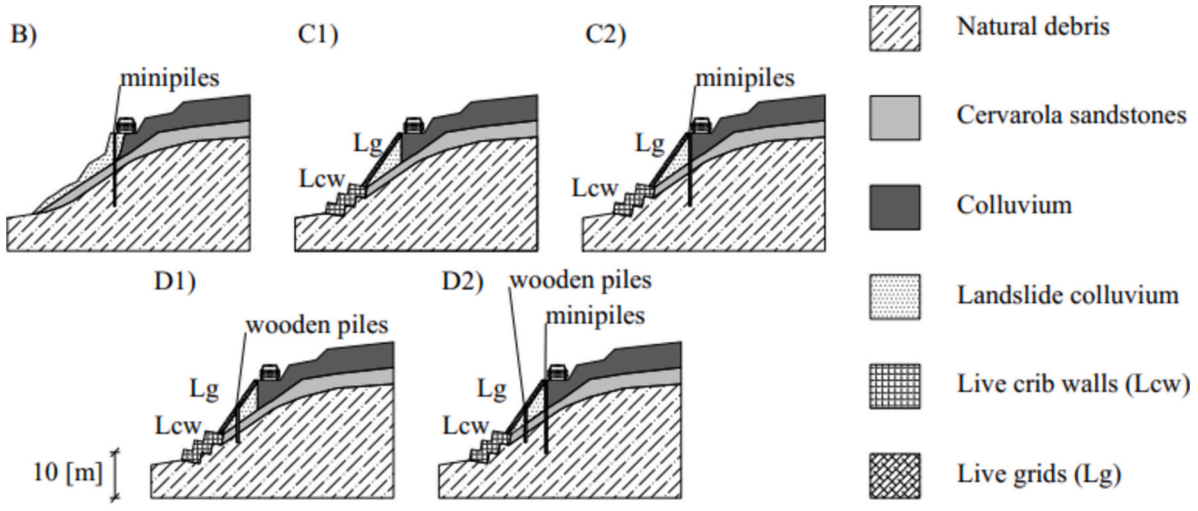

Fig. 8. Schematic overview of technological solutions: B) stabilization with minipiles (gray solution); C1) stabilization with live crib walls and live grids (green solution); C2) stabilization with minipiles live crib walls and live grids (combined solution); D1) stabilization with wooden piles live crib walls and live grids (green solution); D2) stabilization with minipiles wooden piles live crib walls and live grids (combined solution). (For interpretation of the references to color in this figure legend, the reader is referred to the web version of this article.)

the non-deterministic load-resistance factor design (LRFD) format. LRFD-based design relies on the assignment of characteristic values and partial factors. These assignments are aimed at ensuring the target reliability of the system in terms of probability of attaining a specific set of limit states.

While partial factors are tabulated, characteristic values must be assigned by designers. However, the definition of characteristic values according to Eurocode 7 EN 1997–1:2004 (CEN, 2004) and compliant National Regulations such as the Italian NTC2018 (MIT, 2018) is not univocal. In principle, the characteristic value of a parameter should be selected using statistical processing of data from in-situ and/or laboratory testing on the basis of the magnitude and relevance of the spatial variability of that parameter in the development of the mechanism related to the evolution of a specific limit state and in a specific spatial direction. Clause §2.4.5.2(2)P of EN 1997–1:2004 states that "the characteristic value of a geotechnical parameter shall be selected as a cautious estimate of the value affecting the occurrence of the limit state." This definition differs from the general, statistical definition of the characteristic value of a structural material as "the 5% fractile value attained in a hypothetical unlimited test series" given in §1.5.4.1 and §4.2(3) Eurocode 0 "Basis of structural design" EN 1990:2002 (CEN, 2002).

The wording "value governing the occurrence of the limit state" acknowledges that there are at least two design situations that must be considered in the choice of the characteristic value. EN 1997–1:2004 §2.4.5.2(7) states that "The zone of ground governing the behavior of a geotechnical structure at a limit state is usually much larger than a test sample or the zone of ground affected in an in-situ test. Consequently, the value of the governing parameter is often the mean of a range of values covering a large surface or volume of the ground. The characteristic value should be a cautious estimate of this mean value", while EN 1997–1:2004 §2.4.5.2(8) states that "If the behavior of the geotechnical structure at the limit state considered is governed by the lowest or highest value of the ground property, the characteristic value should be a cautious estimate of the lowest or highest value occurring in the zone governing the behavior." The first case corresponds to a non-local failure, in which the limit state is governed by a large volume of soil and in which it is presumed that a mean value can be estimated within the large volume of soil. The characteristic value is selected with 95 % confidence in the calculated mean value. The second case refers to a local failure, for which the characteristic value can be selected as the 5 % fractile of the probability density function representing the variability of a single value of the property of interest, no longer of the mean. Both approaches to the selection of the characteristic value are conceptually consistent with the basic definition of the characteristic value. However, from a statistical perspective, they may result in significantly different values even if the calculated mean in the non-local failure case is equal to the mean value of the probability distribution of the point value for the local failure. In design practice, it is most often difficult to assess a priori the relevance of spatial variability and to determine which statistic should be taken as the characteristic value, because such value needs to be defined as an input while, according to the dual definition, it should result from the output modeling of the geotechnical system. This also poses a problem in LEM stability analyses because the location and spatial extension of failure surfaces is not known a priori, and actually depends on the geotechnical model considered in the analysis. Because of this dichotomy, engineers most often assign characteristic values subjectively, thereby forsaking the potential of non-deterministic analyses.

To quantify the effect of the lack of univocity in the definition of the characteristic value and the frequently encountered consequent difficulty in establishing a priori the statistical criteria to assign such value in design, this study involved a parametric sensitivity analysis of the effects of adopting each of the two definitions of characteristic values of shear strength parameters on LEM-calculated factors of safety. The non-local failure case was addressed by considering the aggregate uncertainty present in the modeling scenarios. Aleatory uncertainty was accounted for by modeling the spatial variability of root-induced cohesion and the temporal variability of strength parameters of living materials. Epistemic uncertainties include: (a) measurement uncertainties and the definition of the representative value in a depth range for the effective cohesion and the friction angle of the rooted soil; (b) measurement uncertainties and the selection of the representative value of the cohesion and the wood friction angle; and (c) transformation uncertainty arising from the theoretical nature of the equivalent cohesion calculation model given in Eq. (10). The local failure does not account for the aleatory component of uncertainty resulting from spatial variability.

The assignment of design values was conducted for each non-deterministic parameter through a sequential procedure involving: (1) the selection of suitable probability distribution; (2) the assignment of distribution parameters; (3) the calculation of the cumulative distribution function; and (4) the extraction of characteristic values for the "non-local" failure case, corresponding to the 50 % percentile of the cumulative distribution (hereinafter, "MN"), and for the "local" failure case, corresponding to the 5 % percentile (hereinafter, "QT"). This process was applied to the geotechnical parameters included in the Mohr-Coulomb and Tresca failure criteria; more specifically, friction angle and effective cohesion (Mohr-Coulomb) and undrained strength (Tresca). The uncertainty in unit weight is known to be less relevant and was thus not considered in this study for sake of simplification (e.g., Uzielli et al., 2007).

The CoVs for parameter uncertainty in soil effective cohesion c' and effective friction angle ϕ' were assigned at 0.40 and 0.30, respectively, through a review of technical literature focusing on geotechnical uncertainty (e.g., Uzielli et al., 2007). The CoV for epistemic uncertainty in radical cohesion c_v was assigned at 0.60 through the descriptive statistical processing of experimental data. The CoV of transformation uncertainty for the equivalent lens model used to calculate equivalent parameters was assigned at 0.50. Gaussian distributions were selected for friction angle while log-Gaussian distributions were used for effective cohesion and undrained strength. The difference in the choice of the distribution lies in the smaller central tendency values of effective cohesion and undrained strength which, associated with the high CoV, could lead to sampling negative values which are physically not meaningful. As an example, Fig. 9a and Fig. 9b show, respectively, the Gaussian probability density function and the cumulative distribution function for effective friction angle of the "soil and colluvium" layer, while Fig. 9c and Fig. 9d show the corresponding functions for the log-Gaussian-distributed effective cohesion of the same layer. A more detailed insight into the shortcomings of the current formulation of LRFD design codes and the implications on design is provided in Uzielli (2024). The Authors' direct experience involving frequent requests from practitioners in this regard attests to the importance of addressing this aspect of geotechnical slope stability analysis in a structured manner.

4.4. Modeling scenarios and input parameters

LEM stability analyses were conducted for suitable combinations of technological solutions, temporal stages, and design mode as discussed in previous sections. With respect to suitability, only the temporal stage "t00" was considered for technological solutions A and B, in which NBS are not present and for which, therefore, no temporal variations in mechanical properties are envisaged. All ten temporal stages were investigated for technological solutions C and D, which include NBS. Modeling scenarios are identified by the notation "DESIGN MODE - TECHNOLOGICAL SOLUTION.TEMPORAL STAGE". For instance, the notation "QT-C1.t20" refers to technological solution C1 at the temporal stage of 20 years after construction, using parameters pertaining to the QT design mode. The definition of inputs to modeling scenarios is described in the following.

The geometric cross-sections used in the SSAP modeling are shown

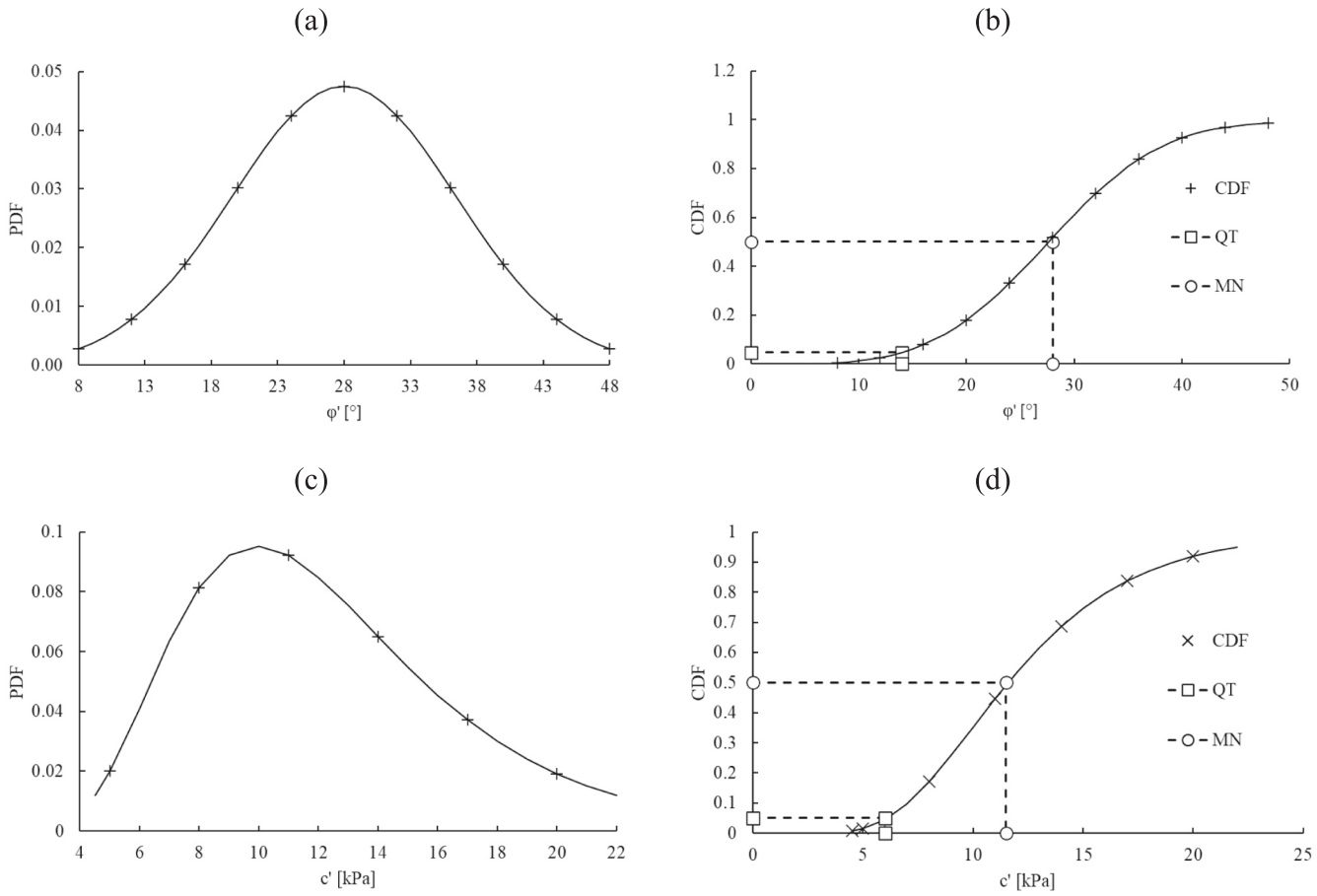

Fig. 9. Example derivation of MN and QT parameter values for: (a) friction angle of the "soil and colluvium" unit - Gaussian probability density function; (b) friction angle of the "soil and colluvium" unit - Gaussian cumulative distribution function with 5 % and 50 % quantiles; (c) effective cohesion of the "soil and colluvium" unit - log-Gaussian probability density function; (d) effective cohesion of the "soil and colluvium" unit - log-Gaussian cumulative distribution function with 5 % and 50 % quantiles.

for all scenarios in Fig. 10. As shown in the table at the bottom of the figure, the number of layers required to achieve the geotechnical model varied among scenarios. The definition of layers 6 to 18 allows the modeling of the temporal, depth-wise variation in equivalent cohesion in NBS materials due to root growth and wood decay. Table 1 provides the values of strength, i.e., effective friction angle and effective cohesion (for Mohr-Coulomb materials) or undrained strength (for Tresca materials) by scenario, design mode, and temporal stage. An analogous process was conducted for unit weight. A live load of 12.5 kPa was included in all stability analyses to account for the possible presence of vehicles.

The site-specific application of the approaches to the equivalent geotechnical modeling of the Montisoni site described in Section 3 results in the compilation of Table 1, which details the quantitative values of geomechanical parameters assigned to each of the geometric layers described in the previous section for the t00, t05, t10, t15, t20, and t25 temporal stages. Table 1 allows the appreciation of the spatial and temporal variability of the geomechanical parameters of NBS lenses.

4.5. LEM analysis settings

The SSAP software offers a broad range of modeling options of varying degrees of complexity. In the Montisoni case study, potential critical surfaces were generated using the "random Search" (RS) random generation technique (Siegel et al., 1981). The RS algorithm is suitable for steep and non-homogeneous slopes such as the case study presented herein. In the RS technique, no prior assumptions are made regarding the shape of the sliding surfaces. Samples of 10,000 locally concave-convex composite random surfaces, composed of segments of length 1.00 m, were generated through Monte Carlo Simulation for each of the modeling scenarios. Among the methods available in the SSAP software, the Morgenstern & Price's method (Morgenstern and Price, 1965) was implemented as it is considered as one of the most numerically stable and of general applicability (Chowdhury et al., 2009). A total of 42 stability analyses were performed, with each analysis requiring between 5 and 10 min of computation time due to the varying complexity of the geotechnical models.

5. Presentation and discussion of results

This section provides and discusses critically selected outputs of the stability analyses for the modeling scenarios described in Section 4. In addition to the factor of safety *FS*, which constitutes the typical output of LEM analyses, SSAP is equipped with a complementary methodology which allows the visualization of the spatial distribution of *FS* itself.

5.1. Example outputs

This section presents selected qualitative visual outputs and quantitative statistical outputs of SSAP-based stability analyses. The visual assessment of results is of interest because the green and gray components of the technological solutions contribute to the mechanical performance of the slope in different ways: the former is expected to contribute to stabilization at surficial depths, while the latter should also

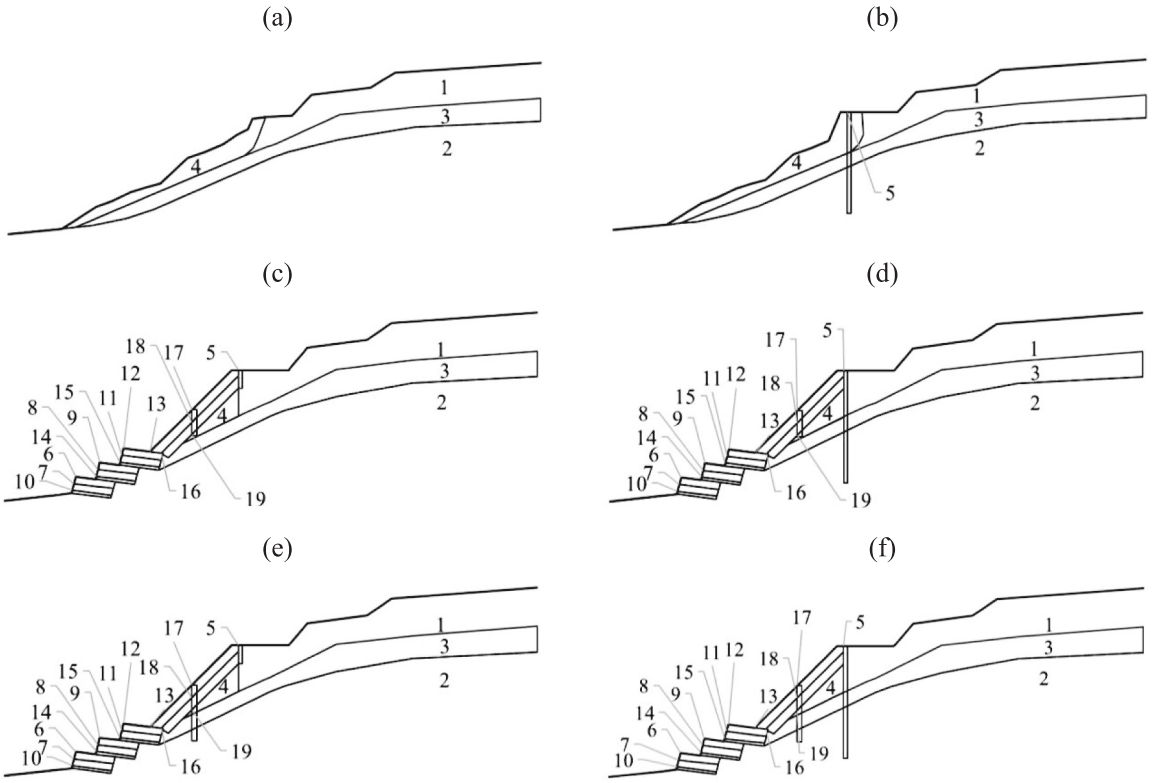

SSAP layer	(a)	(b)	(c)	(d)	(e)	(f)
1	SC	SC	SC	SC	SC	SC
2	DEB	DEB	DEB	DEB	DEB	DEB
3	CER	CER	CER	CER	CER	CER
4	ASC	ASC	ASC	ASC	ASC	ASC
5	-	MIN	SC	MIN	SC	MIN
6	-	-	NBU	NBU	NBU	NBU
7	-	-	NBM	NBM	NBM	NBM
8	-	-	NBM	NBM	NBM	NBM
9	-	-	NBU	NBU	NBU	NBU
10	-	-	NBL	NBL	NBL	NBL
11	-	-	NBM	NBM	NBM	NBM
12	-	-	NBU	NBU	NBU	NBU
13	-	-	NBU	NBU	NBU	NBU
14	-	-	NBL	NBL	NBL	NBL
15	-	-	NBL	NBL	NBL	NBL
16	-	-	NBM	NBM	NBM	NBM
17	-	-	NBU	NBU	WPU	WPU
18	-	-	NBM	NBM	WPM	WPM
19	-	-	ASC	ASC	WPL	WPL

Legend: CER: Cervarola sandstone; ASC: altered soil and colluvium; SC: soil and colluvium; DEB: debris; MIN: minipiles; NBU: nature-based – upper layer; NBM: nature-based – middle layer; NBL: nature-based – lower layer; WPU: wooden pile – surficial layer; WPM: wooden pile – intermediate layer; WPL: wooden pile – bottom layer.

Fig. 10. Geometric assignment of materials in SSAP modeling for technological solutions: (a) A; (b) B; (c) C1; (d) C2; (e) D1; and (f) D2.

improve stability in the less surficial parts of the slope. Statistical outputs are examined in the form of descriptive statistics of the factor of safety against slope instability *FS*. The presentation of visual and parametric results aims to allow the structured comparative assessment of the effects of technological, temporal, and design conservatism-related factors. More specifically, it is of interest to investigate stability in terms of: (1) the effects of technological solutions at the post-event (i.e., pre-construction), end-of-construction, and post-construction temporal stages; and (2) the combined effects of design mode and temporal evolution (i.e., by comparing the outputs of QT and MN scenarios for end-of-

Table 1
Input values of strength parameters for the t00, t05, t10, t15, t20, and t25 temporal stages.

SSAP layer code	Material	Scenario	ϕ'[°]		c',s_u[kPa]						
			Mode	All stages	Mode	All stages					
1, 5	SC (not rooted)	A, B, C1, D1	MN	28.0	MN	11.6					
			QT	14.2	QT	6.2					
2	DEB	All	MN	34.0	MN	31.3					
			QT	17.2	QT	16.6					
3	CER	All	MN	31.0	MN	11.6					
			QT	15.7	QT	6.2					
4, 17, 18, 19	ASC (rooted)	C1, C2	MN	28.0	MN	4.6					
			QT	14.2	QT	2.5					
5	MIN	B, C2, D2	MN	No	MN	467.0					
			QT	no	QT	214.9					
			Mode	All stages	Mode	t_0	t_5	t_{10}	t_{15}	t_{20}	t_{25}
6, 9, 12, 13, 17	NBU	C1, C2	MN	28.0	MN	49.8	68	83	92.6	102.3	112
			QT	14.2	QT	26.3	37	44.5	49.4	54.3	59.2
7, 8, 11, 16, 18	NBM	C1, C2	MN	28.0	MN	49.8	55.4	57.8	59.1	60.3	61.6
			QT	14.2	QT	26.3	30.6	31.7	32.2	32.8	33.4
10, 14, 15	NBL	C1, C2, D1, D2	MN	28.0	MN	49.8	50.3	47.7	45.6	43.5	41.4
			QT	14.2	QT	26.3	28	26.5	25.3	24.2	23.1
17	WPU	D1, D2	MN	no	MN	94	97.6	98	96.4	94.7	93
			QT	no	QT	49.6	58.5	63.7	66.3	68.9	71.5
18	WPM	D1, D2	MN	–	MN	94	91.2	85.1	79.1	73.1	67.1
			QT	–	QT	49.6	52	50.8	49.1	47.4	45.6
19	WPB	D1, D2	MN	–	MN	104.8	95.7	84.7	77.7	68.7	59.7
			QT	–	QT	62	57.2	52.4	47.7	42.9	38.2

Legend: CER: Cervarola sandstone; ASC: altered soil and colluvium; SC: soil and colluvium; DEB: debris; MIN: minipiles; NBU: nature-based – upper layer; NBM: nature-based – middle layer; NBL: nature-based – lower layer; WPU: wooden pile – surficial layer; WPM: wooden pile – intermediate layer; WPL: wooden pile – bottom layer.

construction and post-construction temporal stages, specifically for the as-built technological scenario C2).

5.1.1. Visual outputs

The SSAP software produces and exports multiple visual outputs. Here, two types of outputs are shown; namely: (1) critical slip surfaces; and (2) spatial maps. The first type of visual output, which is the typical result of LEM analyses, is the 2D projection of the most critical, prismatic failure surface (i.e., the surface corresponding to the minimum value of *FS*). The second type of visual output is a raster map (here represented as a grayscale map) providing spatialized values of the "local value" of *FS* calculated from the local stress state, which is computed by SSAP through one of its additional non-LEM features. The two types of output are different because the global *FS* obtained by LEM is related to a specific sliding surface as a whole. Differently, the *FS* raster map, obtained by means of the QFEM (QuasiFEM) method (Borselli, 2023), can discriminate specific zones and the values of *FS* can change along each considered sliding surfaces. Spatial maps thus provide a spatial distribution of instability mechanisms within the slope. The two visual outputs are complementary in allowing a more complete assessment of the stability scenario and a more reliable identification of areas that could generate progressive rupture phenomena. The availability of this integrated information is useful in the preliminary identification of suitable stabilization solutions as well as in the assessment of the performance of design solutions at a more advanced stage of the engineering effort.

Fig. 11 shows the visual outputs described above for the A.t00 (Fig. 11a), B.t00 (Fig. 11b), C1.t00 (Fig. 11c), C2.t00 (Fig. 11d), D1.t00 (Fig. 11e), and D2.t00 (Fig. 11f). modeling scenarios. It should be noted that, strictly speaking, scenarios A and B do not coincide temporally. However, since these scenarios do not include NBS, they are temporally invariant in terms of geometric and geomechanical properties. Scenario A is thus transposed temporally to t00 for simplification. Fig. 11a and Fig. 11b represent, respectively, two typical pre-stabilization and conventional post-stabilization scenarios. It is interesting to note in Fig. 11b that the minimum factor of safety FS_{min}=1.27, which formally satisfies the requirement of Italian design codes, corresponds to a critical failure surface which does not interact with – and is not affected by - the stabilization solution. In this case, therefore, the sole adoption of the conventional solution does not entail a real improvement in safety conditions in the portion of the slope below the minipiles. Visual inspection of Fig. 11 also indicates that the technological scenarios C2 and D2 represent substantial improvements in terms of stability over C1 and D1, respectively.

The assessment of the effects of design mode entails the comparison between the MN and QT scenarios, involving varying degrees of conservatism in the assignment of shear strength parameters of soils. Fig. 12 shows the spatial maps and most critical surfaces for the as-built C2 technological solution for scenarios QT–C2.t00 (Fig. 12a); (b) MN–C2. t00 (Fig. 12b); (c) QT–C2. t10 (Fig. 12c); (d) MN–C2. t10 (Fig. 12d); (e) QT–C2.t25 (Fig. 12e); and (f) MN–C2.t25 Fig. 12f. The pronounced differences between the spatial maps corresponding to different temporal stages attests to the relevance of time in the evolution of geotechnical systems involving NBS. The explicit consideration of this temporal evolution is challenging and fraught with uncertainty from a modeling perspective but allows a significantly more rational insight into the presumable physical behavior of NBS-stabilized systems.

In the temporal transition between scenarios C2.t00 and C2.t25, the critical surfaces extend, reaching the foot of the slope and cutting the last order of piling, due to the increased strength provided by the development of the root system in the superficial layers. It is important to note that critical surfaces are markedly scenario-specific. This observation should come as no surprise, given the complexity of the slope model and the marked effects of the temporal variation in the contributions of the soil-root system and of the wooden materials to the stability of the slope itself.

5.1.2. Statistical outputs

LEM approaches to geotechnical slope stability analyses entail the generation of potential slip surfaces according to a variety of algorithms and the calculation of the factor of safety (*FS*) for each surface according to Eq. (1). Depending on the quality and complexity of the generation algorithm, LEM approaches are capable of replicating the physical complexity of real slopes to varying degrees. However, some degree of epistemic model uncertainty, stemming from factors such as the simplification of the physical reality into a 2D model and the assumptions underlying the calculation of the factor of safety, is inevitably

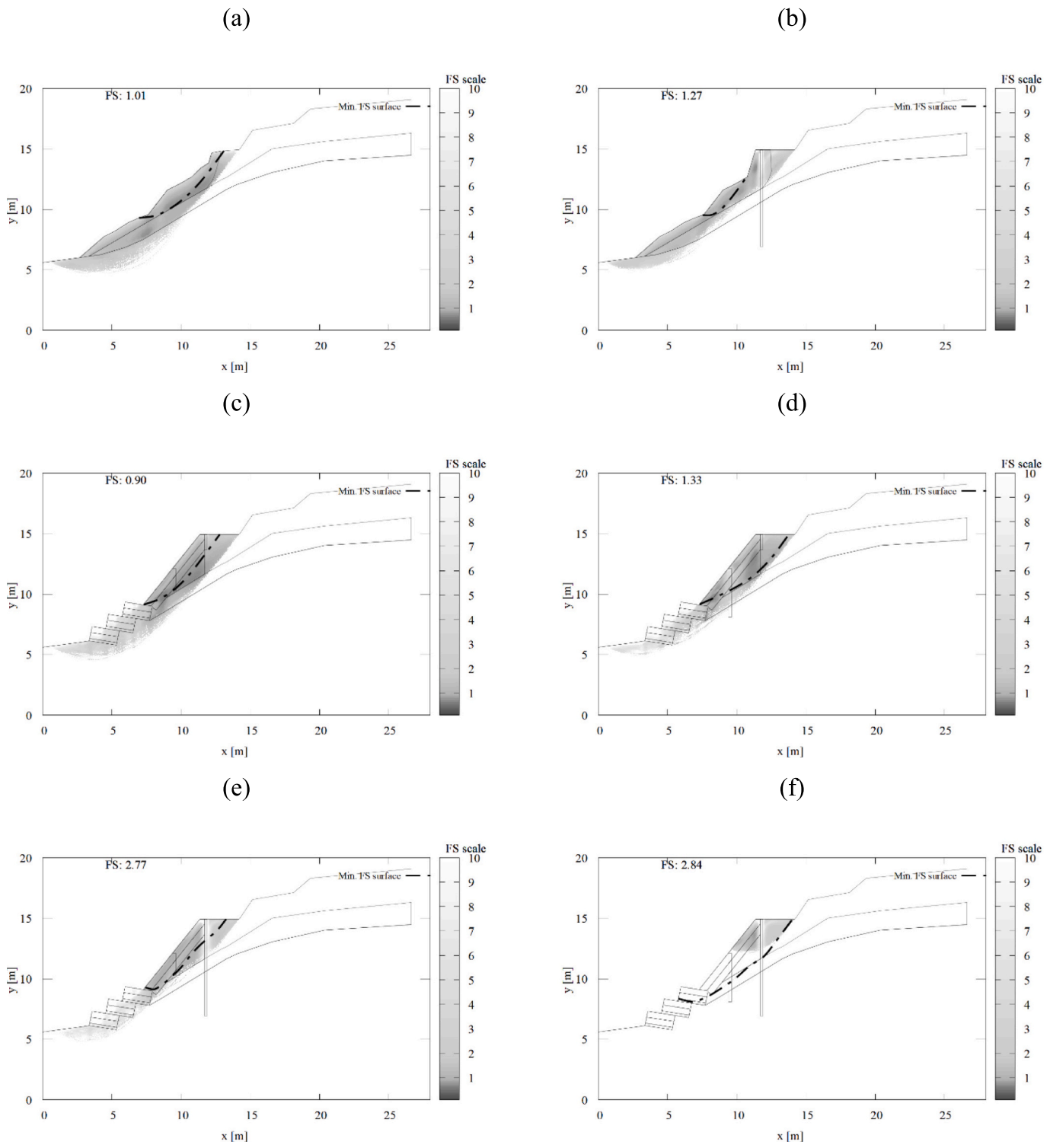

Fig. 11. Spatial maps of *FS* obtained with the QuasiFEM algorithm - (Borselli, 2023) with indication of the most critical sliding surface for design mode MN at time t00 for technological scenarios: (a) A; (b) B; (c) C1; (d) D1; (e) C2; and (f) D2.

introduced. LEM analyses are typically conducted in a deterministic mode, in which only the most critical failure surface is considered and the minimum value of *FS* is extracted. This approach may not be robust, as the single minimum value may correspond to a physically less plausible failure surface. Moreover, such minimum value may differ widely from the values associated with other failure surfaces and may thus introduce bias in the critical assessment of stability. The non-deterministic implementation of LEM analyses, involving the generation of a large number of surfaces and the statistical-probabilistic analysis of the output sample of *FS*, allows a more robust quantitative interpretation and assessment of the stability of a slope because multiple failure scenarios are investigated. In this paper, the variability in samples of *FS* is addressed through a second-moment descriptive statistical analysis. More specifically, the sample containing the bottom 5 % lowest factor of safety among the 10,000 factors obtained (i.e., the 500 lowest values of *FS*) is considered for each modeling scenario. This sub-sample

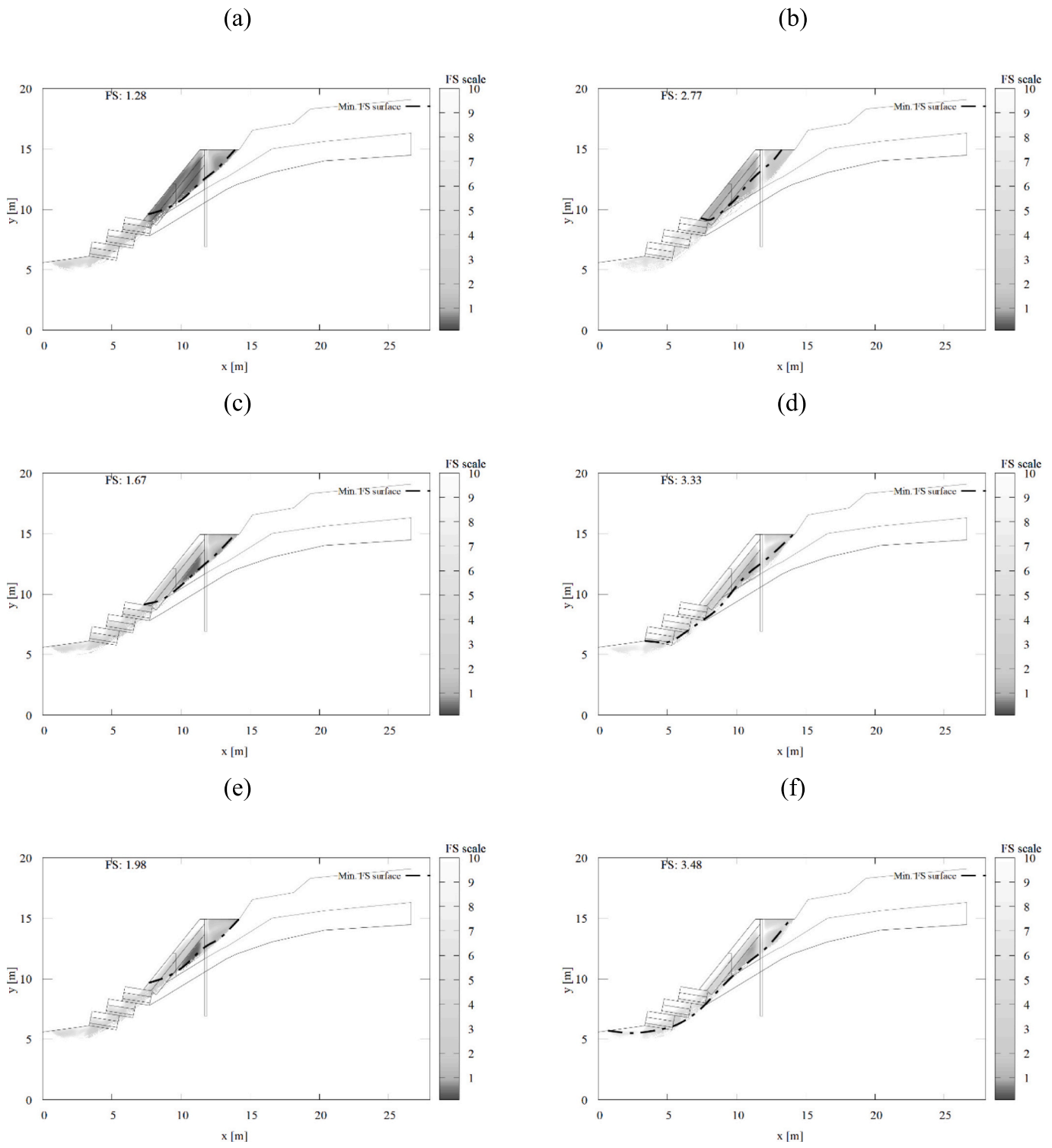

Fig. 12. Spatial maps of *FS* obtained with the QuasiFEM algorithm (Borselli, 2023) for technological scenario C2 with indication of the sliding surface with the lowest FS at: (a) design mode QT – temporal stage t00; (b) design mode MN – temporal stage t00; (c) design mode QT – temporal stage t10; (d) design mode MN – temporal stage t10; (e) design mode QT – temporal stage t25; (f) design mode MN – temporal stage t25.

of *FS* is denoted as FS^* hereinafter. Fig. 13 shows the relative frequency histograms of *FS* (in gray) and the subset FS^* (in black) for the technical solution C1 for the QT design mode and for temporal stages t00 (Fig. 13a) and t05 (Fig. 13b).

The visible difference in the relative frequency histograms attests to the significant change in the distribution of sample values of *FS* and FS^* in favor of stability (i.e., with an almost complete disappearance of values below unity) due to the growth of roots in the surficial layers and despite the partial degradation of wooden elements of live crib walls and live grids. While relative frequency histograms allow the visual appreciation of the temporal variation of the distribution of the factors of safety, it is convenient to conduct quantitative assessments through sample statistics. To enable the quantitative assessment of the dependency of FS^* from technological scenarios, design modes, and tem-

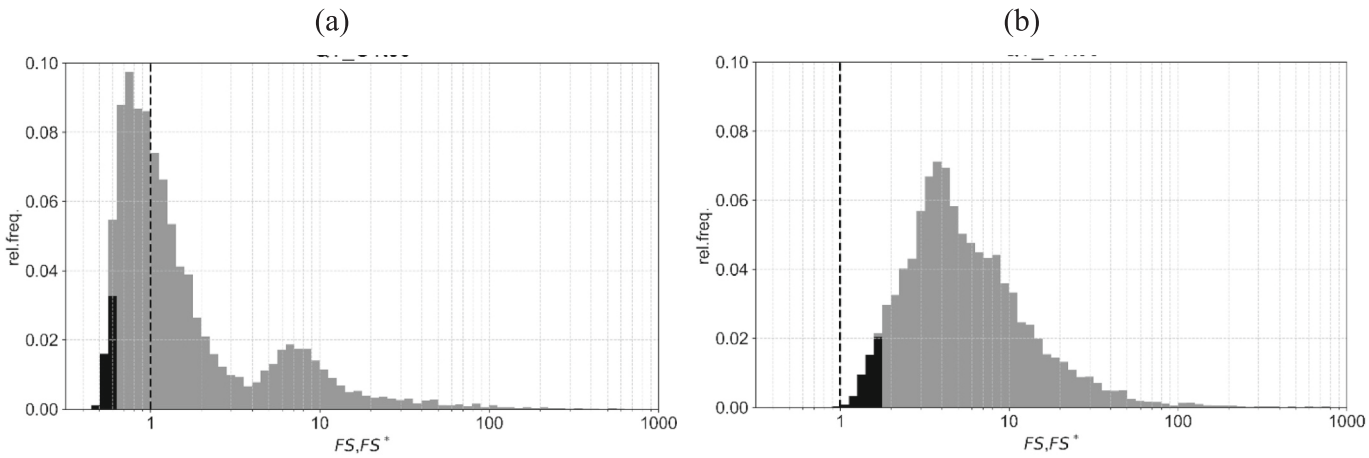

Fig. 13. Relative frequency histograms of FS (in gray) and the lower 5 % subset FS^* (in black) for the technical solution C1 for the QT design mode at temporal stages: (a) t00; and (b) t05.

poral stage, three descriptive sample statistics of FS^* were calculated for each modeling scenario; namely: (1) the sample minimum FS^*_{min}, which corresponds to the absolute sample minimum of FS; (2) the sample mean FS^*_{mean}, which parameterizes the central tendency of FS^*; and (3) the sample coefficient of variation FS^*_{CoV}, which is calculated as the ratio of the sample standard deviation to FS^*_{mean} and which provides a measure of

Table 2
Output sample statistics of the lower-bound sub-sample FS^* of the factor of safety and frequentist probability of stability P_{stab} by modeling scenario.

Technological solution		Temporal stage	Design mode							
			MN				QT			
			FS^*_{min}	FS^*_{mean}	FS^*_{CoV}	P_{stab}	FS^*_{min}	FS^*_{mean}	FS^*_{CoV}	P_{stab}
A		A.t00	1.09	1.28	0.047	1.0000	0.58	0.70	0.057	0.7986
B		B.t00	1.27	1.68	0.071	1.0000	0.74	0.97	0.082	0.9710
C	C1	C1.t00	0.91	1.07	0.047	0.9936	0.48	0.57	0.053	0.5698
		C1.t01	1.47	2.22	0.099	1.0000	0.86	1.41	0.121	0.9992
		C1.t02	1.54	2.26	0.097	1.0000	0.92	1.46	0.116	0.9995
		C1.t03	1.53	2.25	0.098	1.0000	0.90	1.47	0.122	0.9997
		C1.t04	1.56	2.28	0.092	1.0000	0.94	1.48	0.122	0.9997
		C1.t05	1.56	2.31	0.095	1.0000	0.93	1.51	0.119	0.9996
		C1.t10	1.77	2.46	0.102	1.0000	0.98	1.60	0.125	0.9999
		C1.t15	1.77	2.53	0.099	1.0000	1.06	1.67	0.132	1.0000
		C1.t20	1.83	2.57	0.101	1.0000	1.10	1.73	0.133	1.0000
		C1.t25	1.84	2.67	0.109	1.0000	1.10	1.83	0.126	1.0000
	C2	C2.t00	2.77	3.67	0.074	1.0000	1.28	1.63	0.074	1.0000
		C2.t01	3.16	5.50	0.109	1.0000	1.70	2.63	0.110	1.0000
		C2.t02	3.22	5.49	0.118	1.0000	1.64	2.62	0.107	1.0000
		C2.t03	3.22	5.56	0.115	1.0000	1.63	2.64	0.114	1.0000
		C2.t04	3.27	5.55	0.121	1.0000	1.59	2.72	0.114	1.0000
		C2.t05	3.29	5.65	0.113	1.0000	1.63	2.74	0.109	1.0000
		C2.t10	3.33	5.84	0.128	1.0000	1.68	2.84	0.123	1.0000
		C2.t15	3.36	5.91	0.135	1.0000	1.79	2.99	0.120	1.0000
		C2.t20	3.36	6.07	0.127	1.0000	1.87	3.01	0.126	1.0000
		C2.t25	3.48	6.33	0.125	1.0000	1.98	3.13	0.125	1.0000
D	D1	D1.t00	1.33	1.48	0.034	1.0000	0.66	0.76	0.039	0.6907
		D1.t01	2.13	2.95	0.071	1.0000	1.23	1.66	0.078	1.0000
		D1.t02	2.13	2.99	0.074	1.0000	1.28	1.66	0.072	1.0000
		D1.t03	2.13	3.03	0.073	1.0000	1.25	1.71	0.076	1.0000
		D1.t04	2.24	3.08	0.075	1.0000	1.37	1.71	0.076	1.0000
		D1.t05	2.26	3.13	0.073	1.0000	1.34	1.74	0.080	1.0000
		D1.t10	2.46	3.34	0.087	1.0000	1.33	1.87	0.080	1.0000
		D1.t15	2.47	3.43	0.085	1.0000	1.40	1.95	0.082	1.0000
		D1.t20	2.51	3.59	0.095	1.0000	1.47	2.06	0.083	1.0000
		D1.t25	2.46	3.78	0.090	1.0000	1.44	2.10	0.086	1.0000
	D2	D2.t00	2.85	4.56	0.057	1.0000	1.18	1.53	0.072	1.0000
		D2.t01	3.20	4.81	0.096	1.0000	1.65	2.58	0.093	1.0000
		D2.t02	3.25	4.89	0.090	1.0000	1.70	2.58	0.089	1.0000
		D2.t03	3.33	4.97	0.101	1.0000	1.83	2.65	0.094	1.0000
		D2.t04	3.37	5.04	0.099	1.0000	1.89	2.66	0.098	1.0000
		D2.t05	3.39	5.06	0.095	1.0000	1.88	2.69	0.089	1.0000
		D2.t10	3.73	5.35	0.095	1.0000	1.98	2.80	0.093	1.0000
		D2.t15	3.76	5.47	0.101	1.0000	2.03	2.90	0.097	1.0000
		D2.t20	3.98	5.69	0.093	1.0000	2.05	2.99	0.087	1.0000
		D2.t25	3.68	5.77	0.104	1.0000	2.09	3.06	0.095	1.0000

the dispersion of sample values of FS^* around FS^*_{mean} itself. The adoption of a statistical approach circumvents the possible bias resulting from focusing solely on the minimum value of FS which, in statistical terms, could prove to be an outlier. Moreover, focusing on the 5 % lower-bound sample is conceptually associated with the definition of the characteristic value given in Eurocode 7 and reflects an engineering approach which operates according to rationally conservative estimates. Table 2 contains the output sample statistics of the lower-bound sub-sample of the factor of safety, organized by modeling scenario. The table also provides P_{stab}, the percentage of surfaces for which $FS>1$. This statistic is, in effect, a frequentist estimation of reliability if it is assumed that the boundary between performance and non-performance states is $FS=1$. Fig. 14 illustrates the temporal variation of sample statistics of FS^*. More specifically, Fig. 14a, Fig. 14c, and Fig. 14e refer to FS^*_{min}, FS^*_{mean}, and FS^*_{CoV}, respectively, for design mode MN, while Fig. 14b, Fig. 14d, and Fig. 14f refer to FS^*_{min}, FS^*_{mean}, and FS^*_{CoV}, respectively, for design mode QT. Note that statistics are calculated at discrete time stages and connecting lines are included in the plot solely to allow the enhanced visual inspection of their temporal variation.

5.2. Discussion of results

Inspection of the results presented in the tables and figures in the previous section allows the conduction of a wide range of quantitative assessments, including those corresponding to the ones conducted qualitatively in the previous section. Some notable observations, among the many others which could be made, are reported and discussed in the following.

5.2.1. Which design mode is "correct"?

For all technological scenarios and temporal stages, FS^*_{min} and FS^*_{mean} are significantly smaller for the QT design mode with respect to the MN design mode. This result is to be fully expected, given that QT-related values are more conservative than MN values. On the contrary, FS^*_{CoV} values are smaller for MN scenarios than for QT scenarios. The sample mean, coefficient of variation, minimum, and maximum of the ratios of sample statistics of for the MN scenarios to the QT scenarios (for

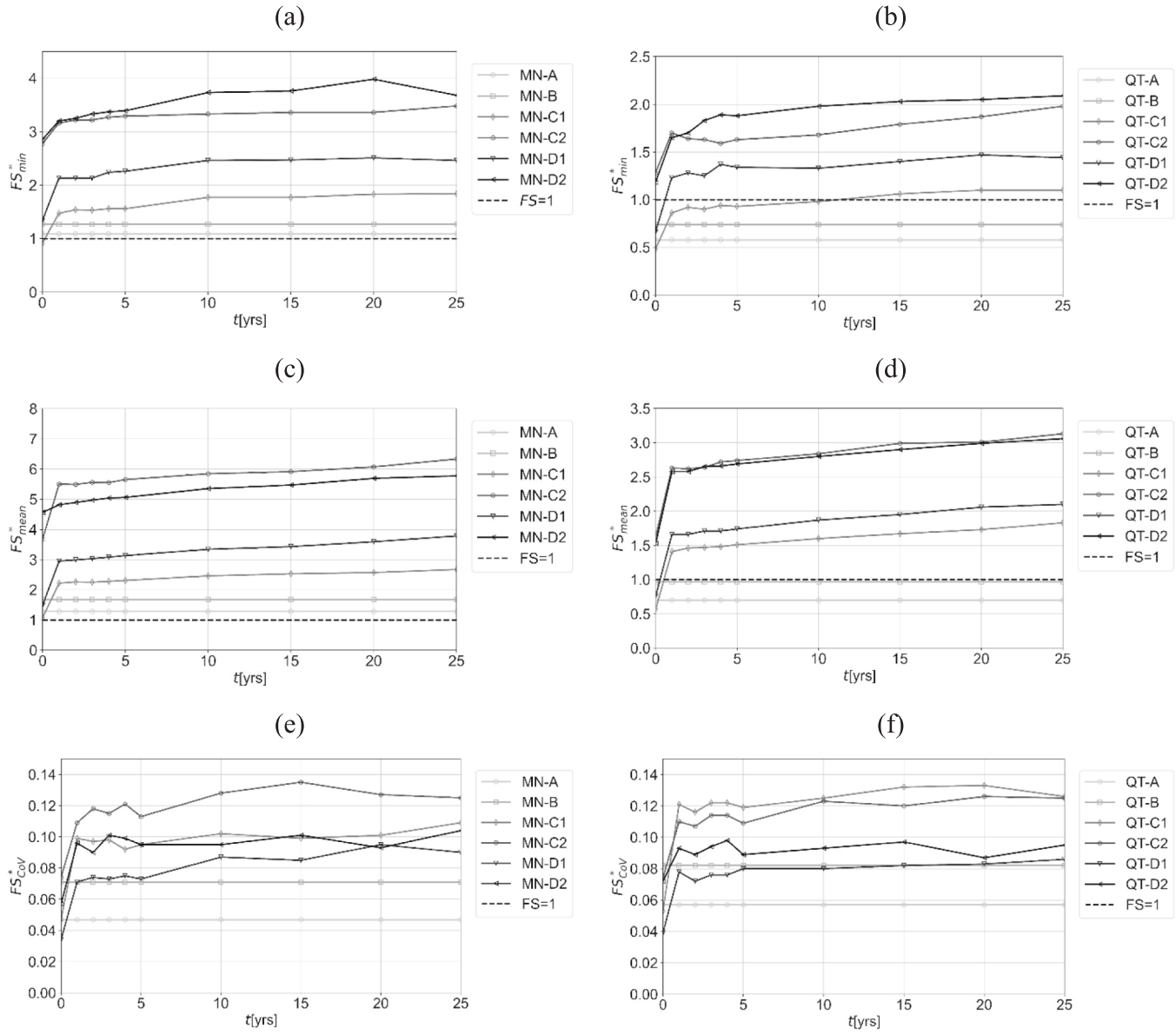

Fig. 14. Temporal variation of sample statistics of FS^*: (a) FS^*_{min} for design mode MN; (b) FS^*_{min} for design mode QT; (c) FS^*_{mean} for design mode MN; (d) FS^*_{mean} for design mode QT; (e) FS^*_{CoV} for design mode MN; (f) FS^*_{CoV} for design mode QT.

corresponding technical scenarios and temporal stages) are given in Table 3. It is worth noting that the coefficients of variation of the MN/QT ratios are limited in magnitude, indicating a relatively small dispersion around mean values.

Given the high variability in outputs between MN and QT scenarios, which design mode is more meaningful? As mentioned previously, the choice of representative values in LRFD is, in principle, related to the expected effect of the relative magnitude of the spatial variability of a parameter with respect to the spatial extension of a failure mechanism for a given limit state. Such extension can vary greatly depending on the geometric and geomechanical attributes of the geotechnical model. As shown in the spatial maps presented in Fig. 11and Fig. 12, failure surfaces tend to be spatially larger with respect to typical magnitudes of spatial variability for shear strength parameters. Consequently, among the two definitions of the characteristic values given in Eurocode 7, the adoption of a "non-local failure" scenario, conceptually amenable to the MN approach, appears to be more suitable than a "local failure" scenario, amenable to the QT approach. In this study, the concept of spatial variability has been implemented in the depth-wise modeling of the effects of root cohesion. However, the rigorous quantitative estimation and representation of spatial variability of geomechanical parameters is a complex topic which cannot be duly addressed in LEM analyses. Such rigorous modeling could result in failure surfaces which are significantly different from those obtained and presented in this paper. This substantial indetermination is a typical example of the limitations of LRFD design modes. As discussed in Uzielli (2024), the adoption of fully probabilistic approaches allows a more univocal investigation and assessment of the performance of geotechnical systems.

5.2.2. Temporal efficacy of NBS solutions

The significant effects of time on slope stability are well-noted and have been widely described in this paper. However, it is relevant to speculate about the implications of the temporal progression of stability on the engineering approach to be adopted: how quickly do NBS contribute to attaining sufficient stability? Can engineers rely on the contribution of rooted soils in the short term? Visual outputs such as those shown in Fig. 14 and statistical outputs given in Table 2 provide useful information about the temporal variation in efficacy of NBS when used alone or with complementary conventional solutions. For technological scenario C1, for instance, in which only NBS are implemented, the relative frequency histogram of FS and the high percentage of unsafe cases attest to an insufficient level of reliability in an engineering perspective. However, this reliability increases very significantly in just one year. As shown in Table 2 and Fig. 14, FS^*_{min} and FS^*_{mean} increase rapidly from t00 to t01 and, subsequently, display less rapidly increasing temporal trends. This observation provides an interesting insight and could be helpful or relevant from a design perspective. Despite this rapid increase in satisfactory performance, the adoption of solution C1 would not provide an acceptable engineering solution since stability would not be sufficiently ensured at the post-construction stage in absence of further short-term stabilization solutions for surficial layers.

5.2.3. The synergy of "quality" and "quantity"

The visual and statistical outputs are complementary, and not redundant, in allowing the integrated assessment of stability. Visual outputs alone cannot provide a direct, quantitative indication of the level of safety as parameterized by the factor of safety; rather, they can only inform about the geometry of failure surfaces. Statistical outputs, on the other hand, can provide interesting insights and supporting information regarding the variability of the factors of safety pertaining to the multiple failure surfaces generated by LEM analyses. For instance, inspection of Table 2 and Fig. 14 allows (at least) two interesting insights. First, values of FS^*_{CoV} are small for all modeling scenarios, indicating a generally low level of dispersion of sample values around FS^*_{mean}. However, inspection of the FS^*_{mean}/FS^*_{min} ratios (ranging from a sample minimum of 1.11 to a sample maximum of 1.82 with a sample mean of 1.49 and a sample CoV of 0.112 for the MN design mode and from a minimum of 1.15 to a maximum of 1.71 with a mean of 1.48 and a CoV of 0.104 for the QT design mode) reveals that these ratios are overall quite high. Minimum values could thus be considered as statistical outliers and their use as sole indicators of stability for any given modeling scenario would not seem appropriate. Second, values of FS^*_{CoV} are smaller at the end of construction, increase rapidly from t00 to t01, and thereafter remain stable or show relatively weakly increasing trends over subsequent temporal stages. In other words, the rapid increasing contribution of roots to stability from t00 to t01 corresponds to a greater dispersion in samples of FS^* around the respective values of FS^*_{mean}. This observation could be related to the increased spatial variability and spatial anisotropy of mechanical properties and the consequent increased variability in the geometry of failure surfaces with low values of FS. Notwithstanding the very interesting implications and leads for further insight provided by Quantitative statistics cannot, by themselves, provide support to the interpretation of the most critical failure mechanisms stemming from the application of the stability analysis approach to a specific geotechnical model. Good practice should involve the integrated assessment to ensure that the choice of a stabilization solution occurs on the basis of sound engineering reasoning and with the support of preferable non-deterministic approaches involving statistics of the factor of safety rather than the sole minimum value. Both visual and statistical outputs depend on the specific combination of geotechnical model and stability modeling approach. While the magnitude of model uncertainty could only be estimated through back-analysis on pre-failure scenarios, it is possible (and warranted) to conduct a parametric investigation on the sensitivity of outputs not only to the relevant factors addressed in this study (technology, design mode, temporal variability) but also to stability modeling options (surface generation algorithm, stability analysis method, etc.).

Table 3
Statistics of ratios of sample statistics of FS^* between MN and QT modeling scenarios.

ratio	mean	CoV	minimum	maximum
$FS^*_{min,MN}/FS^*_{min,QT}$	1.83	0.087	1.64	2.42
$FS^*_{mean,MN}/FS^*_{mean,QT}$	1.85	0.143	1.46	2.98
$FS^*_{CoV,MN}/FS^*_{CoV,QT}$	0.96	0.119	0.75	1.14

6. Concluding remarks and future perspectives

The application of the LEM stability analysis approach to a wide range of modeling scenarios revealed several aspects of considerable geotechnical interest, allowing for the qualitative and quantitative examination of the effects of (1) the geotechnical stabilization technology solution adopted; (2) the temporal variation in the geotechnical properties of the system following from the use of NBS; and (3) the selection of values of strength parameters corresponding to different levels of conservatism. The analyses performed in this study can be conducted routinely in geotechnical practice because they are computationally efficient, with each analysis only requiring 5 minutes on a standard laptop. The inclusion of multiple geotechnical models should not be seen as an academic exercise; rather, geotechnical practice should typically involve the comparative assessment of different solutions to ensure that a suitable, cost-effective, and performing design scenario is selected. Moreover, the necessity to perform multiple analyses in regulatory contexts involving LRFD design formats also stems from the non-univocal definition of characteristic values. Assessing comparatively the outputs pertaining to characteristic values for local- and non-local failure cases allows investigating the sensitivity of design to input values.

The stability analyses conducted for the Montisoni case-study

confirm that NBS can provide a valuable aid for geotechnical slope stabilization. However, the volumes of soil affected by rooting are limited to surficial layers. Moreover, in the scenarios corresponding to the time of construction, the scenarios corresponding to the sole use of NBS, without the use of conventional solutions, do not ensure sufficiently high reliability levels with respect to stability.

The combined solution, actually built at the case study site, thus represents an optimal synthesis from the dual perspective of environmental sustainability and engineering performance. The reprofiling of the intermediate and downslope areas of the slope by means of NBS and the rooting of soils are aimed at ensuring the progressive temporal increase of mechanical strength despite the degradation of the wooden elements of the live crib walls and the live grids. This result is in line with literature studies (e.g., Preti, 2013; Preti et al., 2022a, 2022b).

From the perspective of the design mode, the evaluation of the effects of the different degrees of conservatism in the design values of the parameters of shear resistance confirmed the importance of recognizing and suitably accounting for the presence of significant epistemic uncertainties. Thus, it is essential to rationally define these values according to the design principles compatible with the LRFD methods, such as those included in the structural Eurocodes.

The results of the Montisoni study are case-specific. Case-specificity, which is a common trait of geotechnical analyses, stems from the geometric and geomechanical unicity of sites as well as from the representation of such unicity in the modeling process. The adoption of different modeling options (e.g., the slip surface search algorithm, limit equilibrium method) may produce varying consequences depending on site geometry and geotechnical properties. The LEM analyses conducted using the SSAP software relied uniformly on the Random Search algorithm for the generation of slip surfaces and on the Morgenstern & Price method for the calculation of the factor of safety. The adoption of other surface generation algorithms and stability calculation methods among those available in SSAP would have arguably resulted in different outputs. The comparative application of multiple well-established LEM methods (e.g., Spencer, Sarma, Morgenstern-Price, Janbu, etc.) does not normally lead to appreciable differences. For design purposes it is common to use the Spencer or Morgenstern-Price methods as these have widely proven to be the stable ones from a numerical computational perspective. Algorithms for the generation of potentially unstable surfaces can have, in particular cases, greater influence in the final result (Borselli, 2023). However, considering the objectives of this article, we decided not to extend this point and to defer dedicated analyses to future research. The Freeware SSAP software has confirmed its potential and its flexibility in this application. This confirms what emerges from the wealth of worldwide applications and scientific literature pertaining to the geotechnical and the earth sciences disciplines which can be consulted on the software website.

On a more general note, given the relatively recent surge in interest in NBS on the part of the geotechnical community, there is vast space for improvement in the equivalent geotechnical modeling of NBS and conventional materials, relying for instance on data regarding the durability of structural wood which are available to the authors. This paper proposes an approach which can and should be refined through further dedicated research. Its purpose is intended to be more methodological than output-oriented. Moreover, while this study focused solely on analyses in static conditions, geotechnical slope stability analyses are typically conducted for seismic scenarios adopting a pseudo-static approach. Notwithstanding the scope of the study and the current state of knowledge, the results of this paper are promising. While qualitative and quantitative outputs are not uncritically exportable to other cases, the observed trends in terms of the effects of technological solution, temporal variability, and level of design conservatism are consistent with geotechnical theory, experience, and critical reasoning. This observation sets an encouraging basis for future advancements.

Environmental requalification should not be seen as the sole driver of a more frequent use of NBS and combined solutions. Construction costs for these solutions may prove to be appreciably lower with respect to those of conventional solutions, thereby facilitating their implementation in a wider range of countries. The solution adopted in the present case study allowed the Administration of the Municipality which hosts the Montisoni site to successfully fulfill the goal of road stabilization with substantially diminished economic effort. As a matter of fact, the site was not easily accessible for big construction machines and the adoption of a more conventional stabilization solution would have required, quite inconveniently given the topographic setting and the environmental value of the area, the construction of a specific temporary road to transport all the necessary equipment. The decision to adopt a SWBE approach involving NBS combined with conventional engineering systems allowed the use of relatively small drilling machines and an excavator. Minipiles were installed using a spacing greater than three times their diameter, without having the risk of soil flowing between them. In fact, the presence of the NBS downhill of the minipiles guarantees the effective retaining of the soil, especially as the rooting system develops over time. It is worth noting that the construction of NBS structures requires specific practical expertise by construction companies. Unfortunately, such expertise is currently not widespread among general contractors. The use of a combined solution allowed to reduce the number of minipiles by 50 % with respect to the conventional-only stabilization scenario. These aspects related to logistics and design allowed an overall reduction in construction costs of approximately 25 %.

Along with the improvement in environmental compatibility, cost-performance optimization provides a further relevant motivation for the geotechnical community to resort to NBS and hybrid solutions. Hopefully, this paper may provide a stimulating contribution to advocating an increased awareness of the engineering potential as well as of the environmental and financial advantages of non-conventional approaches to slope stabilization. This awareness, as well as any consequent advancement in method and technology, cannot prescind from the constructive and mutually respectful synergy between disciplines, both in the academic and practitioner communities. Geotechnics alone cannot duly and optimally address and solve problems which require empirical, experimental, and theoretical competence about the mechanical and biological attributes of living materials which constitute nature-based solutions. In this regard, this paper also wishes to provide a concrete example of the positive outcomes of multidisciplinary interaction.

CRediT authorship contribution statement

Marco Uzielli: Writing – review & editing, Writing – original draft, Visualization, Validation, Supervision, Software, Project administration, Methodology, Investigation, Formal analysis, Data curation, Conceptualization. **Andrea Geppetti:** Writing – review & editing, Writing – original draft, Investigation, Formal analysis, Data curation. **Lorenzo Borselli:** Writing – review & editing, Writing – original draft, Software, Methodology, Investigation, Formal analysis, Data curation, Conceptualization. **Stefano Renzi:** Writing – review & editing, Writing – original draft, Formal analysis, Data curation, Conceptualization. **Federico Preti:** Writing – review & editing, Writing – original draft, Validation, Supervision, Methodology, Investigation, Formal analysis, Conceptualization.

Declaration of competing interest

The authors declare that they have no known competing financial interests or personal relationships that could have appeared to influence the work reported in this paper.

Acknowledgements

The Authors wish to gratefully acknowledge: Dr. Daniela Boni for

providing initial examples of SSAP modeling of the Montisoni site; Prof. Luca Uzielli for his useful inputs to the equivalent modeling of the shear strength of structural wood; Georisk Engineering S.r.l. for allowing the use of data and information from the Montisoni case study; the Comune di Bagno a Ripoli for authorizing the realization of the Montisoni case study and allowing its dissemination. This research was partially funded by the Horizon Europe project ARAGORN under grant agreement 101112723.

Data availability

Data will be made available on request.

References

Acharya, M.S., 2018. Analytical Approach to Design Vegetative Crib Walls. Geotech. Geol. Eng. 36, 483–496. https://doi.org/10.1007/s10706-017-0342-5.

Anderson, C.C., Renaud, F.G., Hanscomb, S., Gonzalez-Ollauri, A., 2022. Green, hybrid, or grey disaster risk reduction measures: what shapes public preferences for nature-based solutions? J. Environ. Manag. 310. https://doi.org/10.1016/j.jenvman.2022.114727. Article 114727.

Arnone, E., Caracciolo, D., Noto, L.V., Preti, F., Bras, R.L., 2016. Modeling the hydrological and mechanical effect of roots on shallow landslides. Water Resour. Res. 52 (11), 8590–8612. https://doi.org/10.1002/2015WR018227.

Bischetti, G.B., De Cesare, G., Mickovski, S.B., Rauch, H.P., Schwarz, M., Stangl, R., 2021. Design and temporal issues in Soil Bioengineering structures for the stabilization of shallow soil movements. Ecol. Eng. 169, 106309. https://doi.org/10.1016/j.ecoleng.2021.106309.

Boni, D., 2022. Analisi comparativa di stabilizzazione di pendii con soluzioni convenzionali, naturali e combinate (Comparative analysis of slope stabilization with conventional, nature-based, and combined solutions). Undergraduate Dissertation, Department of Civil and Environmental Engineering, University of Florence (in Italian).

Borselli, L., 2023. SSAP 5.2 - SLOPE STABILITY ANALYSIS PROGRAM″. User manual. https://doi.org/10.13140/RG.2.2.19931.03361.

Capobianco, V., Uzielli, M., Kalsnes, B., Choi, J.C., Strout, J.M., von der Tann, L., Steinholt, I.H., Solheim, A., Nadim, F., Lacasse, S., 2022. Recent innovations in the LaRiMiT risk mitigation tool: implementing a novel methodology for expert scoring and extending the database to include nature-based solutions. Landslides 19, 1563–1583. https://doi.org/10.1007/s10346-022-01855-1.

CEN - European Committee for Standardization, 2002. EN 1990:2002 - Eurocode 0 "Basis of Structural Design". CEN, Bruxelles, Belgium.

CEN - European Committee for Standardization, 2004. EN 1997–1:2004 - Eurocode 7 "Geotechnical design – Part 1: general rules". CEN, Bruxelles, Belgium.

CEN - European Committee for Standardization, 2005. EN 1993-1-1:2005 - Eurocode 3 "Design of Steel Structures - Part 1–1: General Rules and Rules for Buildings". CEN, Bruxelles, Belgium.

Chowdhury, R., Flentje, O., Bhattacharya, G., 2009. Geotechnical Slope Analysis. CRC-Press. https://doi.org/10.1201/9780203864203. ISBN: 978–0–415-46974-6.

Duncan, J.M., 1996. State of the art: Limit equilibrium and finite-element analysis of slopes. J. Geotech. Eng. 122 (7), 577–596. https://doi.org/10.1061/(ASCE)0733-9410(1996)122:7(577.

Fatahi, B., Khabbaz, H., Indradatna, B., 2010. Bioengineering ground improvement considering root water uptake model. Ecol. Eng. 36 (2), 222–229. https://doi.org/10.1016/j.ecoleng.2008.12.027.

Gariano, S.L., Guzzetti, F., 2016. Landslides in a changing climate. Earth Sci. Rev. 162, 227–252. https://doi.org/10.1016/j.earscirev.2016.08.011.

Giachi, E., Giambastiani, Y., Giannetti, F., Dani, A., Preti, F., 2024. Root system evolution survey in a multi-approach method for SWBE monitoring: a case study in Tuscany (Italy). Sustainability 16 (10), 4022. https://doi.org/10.3390/su16104022.

Giambastiani, Y., Errico, A., Preti, F., et al., 2021. Indirect root distribution characterization using electrical resistivity tomography in different soil conditions. Urban For. Urban Green. https://doi.org/10.1016/j.ufug.2021.127442, 127442, ISSN 1618–8667.

Gonzalez-Ollauri, A., Hudek, C., Mickovski, S.B., Viglietti, D., Ceretto, N., Freppaz, M., 2021. Describing the vertical root distribution of alpine plants with simple climate, soil, and plant attributes. Catena 203, 105305. https://doi.org/10.1016/j.catena.2021.105305.

Ito, T., Matsui, T., Hong, W.P., 1981. Design method for stabilizing piles against landslide: one row of piles. Soils Found. 21 (1), 21–37. https://doi.org/10.3208/sandf1972.21.21.

Ji, J., Mao, Z., Qu, W., Zhang, Z., 2020. Energy-based fibre bundle model algorithms to predict soil reinforcement by roots. Plant Soil 446, 307–329. https://doi.org/10.1007/s11104-019-04327-z.

Köppen, W., Geiger, R., 1954. Klima der Erde. Gotha, Klett-Perthes.

Lann, T., Bao, H., Lan, H., Zheng, H., Yan, C., Peng, J., 2024. Hydro-mechanical effects of vegetation on slope stability: a review. Sci. Total Environ. 20, 171691. https://doi.org/10.1016/j.scitotenv.2024.171691.

Li, S., Wang, Z., Stutz, H.H., 2023. State-of-the-art review on plant-based solutions for soil improvement. Biogeotechnics 1 (100035). https://doi.org/10.1016/j.bgtech.2023.100035.

Mao, Z., 2022. Root reinforcement models: classification, criticism and perspectives. Plant Soil 472, 17–28. https://doi.org/10.1007/s11104-021-05231-1.

Ministero delle Infrastrutture e dei Trasporti – MIT, 2018. Decreto Ministeriale del 17 gennaio 2018 "Aggiornamento delle Norme tecniche per le costruzioni". Supplemento ordinario alla "Gazzetta Ufficiale", n. 42 del 20 febbraio 2018 – Serie generale (in Italian).

Morgenstern, N.R., Price, V.E., 1965. The analysis of the stability of general slip surfaces. Géotechnique 15, 70–93. https://doi.org/10.7939/R3JS9HF63.

Mugnai, L., 2019. Analisi della durabilità delle opere di ingegneria naturalistica con dendrodensimetro: il caso della Val di Bisenzio. Undergraduate Dissertation,. University of Florence (in Italian).

Murgia, I., Giadrossich, F., Mao, Z., et al., 2022. Modeling shallow landslides and root reinforcement: a review. Ecol. Eng. 181, 106671. https://doi.org/10.1016/j.ecoleng.2022.106671.

National Building Research Organization – NBRO, 2019. Nature-Based Solutions for Landslide Risk Management. World Bank. https://documents1.worldbank.org/curated/fr/769461564040252588/pdf/Nature-Based-Landslide-Risk-Management-Project-in-Sri-Lanka-Guidance-Document-on-the-Use-Nature-Based-Solutions-for-Landslide-Risk-Reduction.pdf.

OpenStreetMap contributors, 2024. OpenStreetMap [Data set]. OpenStreetMap Foundation. Available as open data under the Open Data Commons Open Database License (ODbL) at.

Perugini, F., 2010. Durabilità delle opere di ingegneria naturalistica: indagini sperimentali su elementi strutturali lignei. Undergraduate Dissertation,. University of Florence (in Italian).

Preti, F., 2006. Stabilità dei versanti vegetati. In: Sauli, G., Cornelini, P., Preti, F. (Eds.), Manuale 3 Ingegneria Naturalistica e Sistemazione dei versanti. Regione Lazio (in Italian), Cap, 10, pp. 137–168.

Preti, F., 2013. Forest protection and protection forest: tree root degradation over hydrological shallow landslides triggering. Ecol. Eng. 61, 633–645. https://doi.org/10.1016/j.ecoleng.2012.11.009.

Preti, F., Giadrossich, F., 2009. Root reinforcement and slope bioengineering stabilization by Spanish Broom (Spartium junceum L.). Hydrol. Earth Syst. Sci. 13, 1713–1726. https://doi.org/10.5194/hess-13-1713-2009.

Preti, F., Dani, A., Laio, F., 2010. Root profile assessment by means of hydrological, pedological and above-ground vegetation information for bio-engineering purposes. Ecol. Eng. 36 (3), 305–316.

Preti, F., Togni, M., Dani, A., Perugini, F., 2011. Il potere del tempo - La durabilità degli elementi lignei delle palificate. ACER, pp. 33–37. ISSN1828–4434, 6/2010.

Preti, F., Capobianco, V., Sangalli, P., 2022a. Soil and water bioengineering (SWB) is and has always been a nature-based solution (NBS): a reasoned comparison of terms and definitions. Ecol. Eng. 181, 106687. https://doi.org/10.1016/j.ecoleng.2022.106687.

Preti, F., Dani, A., Noto, L.V., Arnone, E., 2022b. On the Leonardo's rule for the assessment of root profile. Ecol. Eng. 179, 106620. https://doi.org/10.1016/j.ecoleng.2022.106620.

Rey, F., Bifulco, C.C., Bischetti, G.B., et al., 2019. Soil and water bioengineering: Practice and research needs for reconciling natural hazard control and ecological restoration. Sci. Total Environ. 648, 1210–1218, 2019. ISSN 0048–9697. https://doi.org/10.1016/j.scitotenv.2018.08.217.

Romano, N., Lignola, G.P., Brigante, M., Bosso, L., Chirico, G.B., 2016. Residual life and degradation assessment of wood elements used in soil bioengineering structures for slope protection. Ecol. Eng. 90, 498–509. https://doi.org/10.1016/j.ecoleng.2016.01.085.

Sauli, G., Cornelini, P., Preti, F., 2005. Manuale di Ingegneria Naturalistica, vol. 3. Sistemazione dei versanti, Roma (in Italian).

Schwarz, M., Preti, F., Giadrossich, F., et al., 2010. Quantifying the role of vegetation in slope stability: a case study in Tuscany (Italy). Ecol. Eng. 36 (3), 285–291. https://doi.org/10.1016/j.ecoleng.2009.06.014.

Schwarz, M., Giadrossich, F., Cohen, D., 2013. Modeling root reinforcement using a root-failure Weibull survival function. Hydrol. Earth Syst. Sci. 17, 4367–4377. https://doi.org/10.5194/hess-17-4367-2013, 2013.

Selli, L., Guastini, E., 2014. Analytical monitoring of soil bioengineering structures in the Tuscan-Emilian Apennines of Italy. EGU General Assembly 2014. Wien sessionSSS2.10/BG9.7/GM4.8/HS8.3.9/NH3.9.

Siegel, R.A., Kovacs, W.D., Lovell, C.W., 1981. Random surface generation in stability analysis. J. Geotech. Eng. 107 (7), 996–1002.

Stokes, A., Douglas, G.B., Fourcaud, T., et al., 2014. Ecological mitigation of hillslope instability: ten key issues facing researchers and practitioners. Plant Soil 377 (1), 1–23. https://www.jstor.org/stable/44244605.

Tron, S., Dani, A., Laio, F., Preti, F., Ridolfi, L., 2014. Mean root depth estimation at landslide slopes. Ecol. Eng. 69, 118–125. https://doi.org/10.1016/j.ecoleng.2014.03.019.

Uzielli, M., 2024. The role of data in the evolution of geotechnical design. Riv. Italian. Geotec. https://doi.org/10.19199/2024.2.0557-1405.022.

Uzielli, M., Lacasse, S., Nadim, F., Phoon, K.-K. (2007). Soil variability analysis for geotechnical practice. Keynote paper, in T.S. Tan, K.K. Phoon, D.W. Hight & S. Leroueil (eds.), Proceedings of the 2nd International Workshop on Characterisation and Engineering Properties of Natural Soils. Singapore, November 29 – December 1, 2006. The Netherlands: Taylor & Francis (CD-ROM). doi: https://doi.org/10.1201/NOE0415426916.ch3.

Uzielli, M., Rianna, G., Ciervo, F., Mercogliano, P., Eidsvig, U.K., 2018. Temporal evolution of flow-like landslide hazard for a road infrastructure in the municipality of Nocera Inferiore (southern Italy) under the effect of climate change. Nat. Hazards Earth Syst. Sci. 18, 3019–3035. https://doi.org/10.5194/nhess-18-3019-2018.

Varnes, D.J., 1978. Slope movement: Types and processes. In: Landslides: Analysis and Control, Report 176. Transportation Research Board, Washington, pp. 11–33.
Waldron, L.J., 1977. The shear resistance of root-permeated homogeneous and stratified soil. Soil Sci. Soc. Am. J. 41, 843–849. https://doi.org/10.2136/sssaj1977.03615995004100050005x.
Wu, T.H., Mckinnell, W.P., Swanston, D.N., 1979. Strength of tree roots and landslides on Prince of Wales Island, Alaska. Can. Geotech. J. 16, 19–33. https://doi.org/10.1139/t79-003.